

Evaluating the Effects of Organic vs. Conventional Farming on Aquifer Water Quality

Marta Llorente¹ and Marta Suárez²

¹ Departamento de Análisis Económico: Economía Cuantitativa. Universidad Autónoma de Madrid, Campus de Cantoblanco, 28049 Madrid, Spain.

² Departamento de Análisis Económico Aplicado. Universidad de las Palmas de Gran Canaria, Campus Universitario de Tafira, 35017 Gran Canaria, Spain.
Emails: m.llorente@uam.es, marta.suarez@ulpgc.es

Abstract

This study analyzes water quality dynamics and aquifer recharge through irrigated agriculture, contributing to the literature on Managed Aquifer Recharge (MAR) amidst growing water scarcity. We develop two optimal control models—a linear and a non-linear extension of (Martin & Stahn, 2013)—that incorporate the impact of fertilizers on aquifer water quality, distinguishing between organic and conventional farming practices. The linear model applies a constant rebate mechanism, whereas the non-linear model employs a concave rebate scheme. Our results show that, depending on climate change scenarios, fertilizer-induced food price discounts, and pollution levels, a socially optimal equilibrium in fertilizer use can be attained. Policy implications are discussed, emphasizing the trade-off between environmental sustainability and social welfare.

1 Introduction

The optimal management of water resources has become a critical tool in addressing the global challenge of water scarcity. Ensuring the availability and quality of water is not only a pressing environmental issue but also a key objective of the Sustainable Development Goals (SDGs) for the 2030 agenda.

According to the World Bank (2023), approximately 4 billion people currently reside in water-scarce areas, and global water demand is projected to increase by 20-30% by 2050. Climate change exacerbates this issue, with droughts becoming more severe. Between 2000 and 2019, an estimated 1.43 billion people were affected by droughts. Agriculture, which accounts for 70% of global freshwater withdrawals from rivers, lakes, and aquifers, plays a central role in this crisis. Irrigation covers 20% of total agricultural land and contributes to 40% of global food and fodder production. Groundwater, in particular, is a vital resource, with 2 billion people relying on it for their water supply. Effective groundwater management is therefore essential to ensure both food security and water sustainability (World Bank, 2023).

In Spain, the situation mirrors global trends. Data from the Ministry for Ecological Transition and the Demographic Challenge (MITECO) indicate that, as of 2023, 14.6% of the country was under a state of emergency due to water scarcity, while 27.4% was on

alert (MITECO, 2023). Furthermore, by May 2024, Spain’s water reserves had dwindled to just 37% of their capacity (MITECO, 2024).

In this context of escalating climate uncertainty, the sustainable management of water resources —particularly concerning aquifers— has emerged as a critical area of research (Gorelick & Zheng, 2015). The present study addresses an optimal control problem aimed at maximizing social welfare through the efficient allocation of water and food resources derived from aquifers. At its core, this approach emphasizes the sustainable management of these vital resources to ensure long-term societal well-being.

This study introduces two models that apply optimal control theory to groundwater management, with a focus on maximizing social welfare. These models provide a framework for evaluating policies designed to reduce fertilizer use while simultaneously enhancing social welfare within a specific aquifer system.

Building on the foundational work of Martin and Stahn (2013)—which assumed zero fertilizer use, this study extends their aquifer management problem. Section 2.1 provides a detailed overview of the Martin and Stahn model, along with an in-depth exploration of the Managed Aquifer Recharge (MAR) system on which their framework is based. Expanding the scope of existing research, as outlined in Section 2.2, the proposed models integrate fertilizer use and build upon the frameworks established by previous studies (Brock, Xepapadeas, & Yannacopoulos, 2014; Roseta-Palma, 2003; Yadav, 1997).

Fertilizer use in agriculture is known to reduce production costs, leading to lower food prices compared to organic production methods (FAO, 2024; Redlichová, Chmelíková, Blažková, Svobodová, & Vanderpuje, 2021). However, the irrigation of water into aquifers through fertilizer-based crop irrigation also results in the production of polluted water. This necessitates both pumping and purification processes to render the water suitable for human consumption, incurring additional societal costs. Society derives utility from the consumption of water and food, as well as from its preferences regarding the optimal height of the aquifer and environmental quality.

To advance the analysis, this study adopts a methodological framework rooted in optimal control theory. Section 3 formalizes the class of resource management problems under investigation and establishes the necessary first- and second-order optimality conditions derived from Pontryagin’s Maximum Principle and the Arrow sufficiency theorem. These theoretical foundations provide the analytical tools to characterize solutions to the proposed models.

The subsequent sections operationalize this framework: Section 4.1 rigorously defines the aquifer management challenge through a bi-objective optimization lens, balancing agricultural productivity and resource sustainability. Section 4.2 develops two distinct formulations. The first employs a linear price-discount structure to model fertilizer-induced agricultural gains, while the second introduces a concave discount function that better captures diminishing returns and threshold effects observed in real-world systems. Both formulations explicitly incorporate hydrological constraints and socioeconomic trade-offs inherent in groundwater management.

A key assumption underpinning the models is that societal response to water pollution is influenced by nature’s capacity to absorb it. High absorption capacity fosters greater societal patience, while limited capacity leads to impatience, echoing the “tragedy of the commons” articulated by Hardin (1968).

Theoretical solutions for the models are derived in Section 4 using the Maximum Principle. Section 4.3 presents a parametric and equilibria analysis of the Linear Model, identifying conditions under which fertilizer use is socially beneficial and demonstrating

that total fertilizer use can be socially optimal in the absence of significant climate change impacts. In Section 4.4, a similar analysis is conducted for the Non-Linear Model.

Section 5 presents simulations for both the Linear and Non-Linear models, offering a comparative analysis to underscore key differences and insights. Section 5.1 summarizes the effects of varying food rebate values in the Linear Model, while Section 5.2 examines the Non-Linear Model, including the effects of different levels of contamination generated per unit of fertilizer.

The findings in Section 5.3 reveal a trade-off between long-term social welfare and water quality. Notably, social utility tends to be higher when fertilizers are applied at intermediate levels, as opposed to their maximum allowable quantity. To mitigate pollution, policymakers should consider measures to reduce the price gap between organic and conventional products. Such policies could facilitate a socially optimal equilibrium where water quality reaches its maximum potential. However, achieving the highest possible social utility entails accepting certain environmental costs.

This study is not without limitations, as outlined in Section 6. While the developed models effectively capture global social utility, they do not account for the specific interests of key stakeholders, such as farmers, whose preferences significantly influence fertilizer usage decisions (Liu, Bruins, & Heberling, 2018; Pan, He, & Kong, 2020). Parameters used in simulations are chosen to align with Martin and Stahn (2013) ensuring comparability and enabling an evaluation of the models' performance in a generalized context. However, it is important to emphasize that these parameters are not intended to represent any specific real-world scenario, though they can be adapted for such applications. Additionally, in the Non-Linear Model, the equilibrium condition is characterized by an implicit equation that precludes closed-form analytic solutions; thus, we rely on linearization, Hartman's theorem and numerical simulations to characterize the solutions and assess their stability.

The model suggests potential turnpike properties; however, the conditions required for this property to hold, as defined by (Marena & Montrucchio, 1999), are not fully met. Further exploration, including alternative functional forms to refine the modeling of fertilizer benefits, is left for future research.

In summary, Section 2 introduces the problem, reviews relevant literature, and outlines this study's contributions. Section 3 presents the methodology and theoretical framework grounded in optimal control theory. Section 4 formulates and analytically solves the two models that incorporate fertilizer use into aquifer management. Sections 4.3 and 4.4 provide a parametric and equilibrium analysis of both models, identifying conditions under which fertilizer use is socially optimal. Section 5 presents numerical simulations and comparative results: Section 5.1 explores the effect of varying food rebate values in the Linear Model, Section 5.2 analyzes the Non-Linear Model under different pollution intensities, and Section 5.3 highlights the trade-off between long-term social welfare and water quality. Section 6 discusses the study's limitations and outlines directions for future research. Finally, Section 7 concludes the paper.

2 Aquifer management problem

This section establishes the conceptual foundation for subsequent model development. It begins with an analysis of the optimal control framework introduced by Martin and Stahn, which serves as the foundational reference for this study.

The discussion emphasizes the critical integration of water quality parameters in

agricultural management models, particularly through the implementation of Managed Aquifer Recharge (MAR) systems as a mechanism for sustainable groundwater management.

This research extends existing scholarship by systematically addressing aquifer pollution challenges arising from agricultural fertilizer use. Through this analytical lens, the study offers novel insights into the water–agriculture nexus, advancing understanding of coupled human–natural systems in resource management.

2.1 State of the art

Our primary reference is Martin and Stahn (2013), which examines the Crau region in southeastern France through an optimal control framework, demonstrating how surface water irrigation maintains aquifer levels critical for both recreational ecosystems and municipal water supplies. Martin and Stahn’s comparative analysis reveals superior social welfare outcomes under centralized planning (pure water policy setting) versus decentralized management by separate water and agricultural authorities (agri-environmental setting).

While this pioneering study assumes chemical-free agriculture through a Controlled Designation of Origin framework, practical implementations frequently encounter challenges in maintaining zero-input cultivation. Furthermore, the model omits critical water quality parameters, particularly salt and nutrient accumulation from irrigation practices—a significant oversight given that salinization affects 20% of irrigated land globally (FAO, 2021).

Complementing this perspective, Yadav (1997) establishes nitrate pollution as a principal water quality constraint, while Roseta-Palma (2003) develops a generalized framework for water quality management in agricultural systems. Others like Nahorski and Ravn (2000), address pollution modeling in a more general context. These works collectively underscore the necessity of dual quantity-quality optimization in groundwater management.

The methodological framework proposed in this study holds particular relevance for water-scarce regions, where Managed Aquifer Recharge (MAR) systems utilizing alternative water sources—such as rainwater, treated wastewater, desalinated seawater—show significant potential. Several techno-economic analyses (Dillon et al., 2019; Levintal et al., 2023; Page, Bekele, Vanderzalm, & Sidhu, 2018) underscore the importance of MAR systems, and their economic feasibility has been examined by researchers such as Heinz, Salgot, and Dávila (2011); Pavelic et al. (2022).

The models proposed in this study may also prove valuable in such contexts, as they incorporate water impurities and the associated treatment costs, which are critical factors in sustainable water management.

In the Spanish context, where 45% of wastewater is used in agriculture, 36% in parks and recreational areas, 10% in industry and the remaining percentage in street cleaning and other uses (Jodar-Abellan, López-Ortiz, & Melgarejo-Moreno, 2019), our model’s incorporation of impurity could provide critical insights for sustainable reuse strategies. The agricultural sector is the largest recipient of wastewater, highlighting the importance of optimizing its use in this domain.

In selecting an appropriate MAR system, Alam, Borthakur, Ravi, Gebremichael, and Mohanty (2021) recommend that the choice should depend on the properties, availability, and quality of the water in question. This underscores the need to incorporate water

quality as a critical variable in the decision-making process.

The following section details the key aspects of the La Crau problem. For analytical consistency, we adopt the conclusions of Martin and Stahn (2013), which identify the social planner scenario as the optimal outcome.

Specifically, the social utility function employed by Martin and Stahn (2013) is defined as follows:

$$U_0(h_t, f_t, g_t) = s(f_t) + \sigma(h_t, g_t) + e(h_t). \quad (1)$$

The surplus food consumption, represented by $s(f_t)$, is defined as the difference between the willingness to pay for food consumption, represented by the utility function $u(f_t)$, and the cost of purchasing this consumption, given by cf_t , where c represents the unit price of food.

Similarly, the surplus groundwater consumption, denoted by $\sigma(h_t, g_t)$, is defined as the difference between the willingness to pay for the groundwater consumption and the price adjusted to the height of the aquifer, which reflects the associated pumping costs.

The final term, $e(h_t)$, captures an environmental preference. Unlike traditional groundwater management literature (Jean-Christophe, 2020; Roseta-Palma, 2003), this model assumes that consumers derive utility from the height of the aquifer, with an optimal social level denoted by \bar{h} .

Finally, the aquifer dynamics are governed by the following equation, as established by Martin and Stahn:

$$\dot{h}_t = -g_t + bf_t. \quad (2)$$

Equation (2) indicates that the height of the aquifer, h_t , is positively influenced by food production (through recharge mechanisms) and negatively affected by groundwater extraction. The balance between these two factors determines the net change in aquifer height over time.

2.2 Contribution to background literature

Our contribution to the existing literature addresses the issue of chemicals and water quality in agriculture. Water quality is influenced by various factors, including its natural composition and contamination from human activities, such as sewage and industrial pollution. In this context, water used for agricultural irrigation—which recharges the aquifer—can become a source of contamination due to the application of fertilizers. Despite growing concerns regarding their environmental, health, and sustainability impacts, farmers continue to apply these chemicals due to market pressures and limited alternatives (Wilson & Tisdell, 2001).

Furthermore, the use of fertilizers contributes to the generation of pollutants, a process commonly assessed through nitrate concentration levels, a direct byproduct of inorganic fertilizer application on cropland (Bijay-Singh & Craswell, 2021; Singh et al., 2022). Consequently, water must be treated to ensure its safety for human consumption, which introduces a social cost term into the utility function. Equation (3) illustrates how a decline in water quality, represented by the variable Ψ_t , negatively affects social welfare, following a quadratic relationship:

$$\rho(\Psi_t) = -\frac{1}{2}(1 - \Psi_t)^2 \quad (3)$$

In addressing the issue of water pollution, it is important to note that the use of fertilizers—being polluting inputs—tends to lower food prices. Therefore, we assume that fertilizer application results in a decrease in food prices. A distinction is drawn between organic production, which avoids fertilizer use, and conventional production, which relies on them. This choice is justified by several factors. First, organic products incur higher production costs, rendering them more expensive than conventional ones (FAO, 2024). Second, Redlichová et al. (2021) empirically demonstrated in the Czech Republic that conventional farming yields higher production per unit of land and lower energy consumption per unit of product compared to organic farming.

To capture this effect, we modify the functional form of the surplus from food consumption¹ proposed by Martin and Stahn (2013). An additional parameter, β , is introduced to represent the impact of fertilizer use on reducing food prices. As detailed in Section 4, two distinct modeling approaches are employed to analyze the influence of fertilizer use on food pricing. In the first approach, the price reduction is represented as a linear function of the (dimensionless) quantity of pollutant input used at time t , γ_t , implying that the optimal level of fertilizer use for maximizing social welfare is either total or zero, depending on the parameter values. In the second approach, a non-linear model is considered, allowing for intermediate levels of fertilizer use and evaluating optimal social welfare under both scenarios.

These two scenarios are encapsulated in the following modification of the food surplus function:

$$s(f_t, \gamma_t) = u(f_t) - c(\gamma_t)f_t \quad \text{with} \quad \begin{cases} c(\gamma_t) = c - \beta\gamma_t & \text{(Linear case)} \\ c(\gamma_t) = c - \beta\gamma_t^{1/2} & \text{(Non-linear case)} \end{cases} \quad (4)$$

For the remainder of this study, the linear representation of food price discounts resulting from fertilizer use will be referred to as the *Linear Model*, while the concave representation is termed the *Non-Linear Model*.

To capture the dynamics of water quality, we introduce a new equation inspired by Roseta-Palma (2003). This equation describes the rate of change in pollutant concentration over time:

$$\dot{C}_t = C(f_t, \gamma_t) - \delta C_t, \quad (5)$$

where $C(f_t, \gamma_t)$ represents the concentration of contaminants generated during food production as a result of fertilizer use, γ_t denotes the rate of fertilizer application, and δ corresponds to the natural degradation rate of pollutants per unit of time. Accordingly, we adopt the functional form

$$C(f_t, \gamma_t) = \eta f_t \gamma_t,$$

with $C_0 = 0$, where the parameter η serves as a scaling factor quantifying the relationship between food consumption and pollutant generation.

Water quality is defined inversely in terms of pollution as follows:

$$\Psi_t = \Psi_{\max} - C_t = 1 - C_t, \quad (6)$$

with the maximum water purity normalized to one. By combining the equations for pollutant concentration (5) and water quality (6), the evolution of water quality is expressed

¹ $s(f_t) = u(f_t) - cf_t$

as:

$$\dot{\Psi}_t = \delta(1 - \Psi_t) - \eta f_t \gamma_t. \quad (7)$$

This equation highlights the dual effects on water quality: while the degradation of pollutants contributes positively, the use of fertilizers has a detrimental impact.

3 Methodology

This study extends the optimal control framework established by Martin and Stahn (2013), which demonstrates the superiority of centralized decision-making in agri-environmental management. Our principal innovation lies in the explicit incorporation of fertilizer use as a strategic control variable, enabling analysis of its dual impact on agricultural productivity and groundwater quality.

The methodological approach combines analytical optimization with numerical validation. We employ Pontryagin's Maximum Principle adapted to the current-value Hamiltonian framework over an infinite time horizon (see Theorem 1) to derive equilibria and obtain analytical solutions for our infinite-horizon problems. Numerical simulations complement the analytical results, allowing for the characterization of dynamic trajectories. This dual methodology follows established practices in economics focused on the efficient allocation of natural scarce resources (Intriligator, 1975; Sethi, 2019).

3.1 Optimal Control Theory over an Infinite Horizon

The governing optimization problem follows the canonical form for stationary infinite-horizon control (Sethi, 2019, 3.3):

$$\left\{ \begin{array}{l} \max_{u_t \in \mathcal{U}(t)} J = \left\{ \int_0^\infty \phi(x_t, u_t) e^{-\rho t} dt \right\}, \\ \text{subject to:} \\ \dot{x}_t = f(x_t, u_t), \quad x(0) = x_0, \end{array} \right. \quad (8)$$

where $x_t \in \mathbb{R}^n$ represents the state variables, evolving according to the differential equations defined by $\dot{x} = f(x_t, u_t)$, with initial condition $x(0) = x_0$. The control variables $u_t \in \mathcal{U}(t) \subset \mathbb{R}^m$ for $t \in (0, \infty)$, are required to be *admissible* (i.e. piecewise continuous) and constrained by the set $\mathcal{U}(t)$, which typically reflects physical or economic restrictions on the control variables at time t . Both state and control variables are required to be non-negative. The functions $\phi, f : \mathbb{R}^n \times \mathbb{R}^m \times \mathbb{R} \rightarrow \mathbb{R}^n$, are assumed to be continuously differentiable, and the discount factor ρ lies in the range $[0, 1]$.

The solution framework employs the *current-value Hamiltonian*:

$$H(x_t, u_t, \lambda_t) = \phi(x_t, u_t) + \lambda_t f(x_t, u_t), \quad (9)$$

where λ_t denotes the vector of adjoint variables encoding shadow prices of resource stocks. Under the stationary assumption, the state equation, the adjoint equation, and the Hamiltonian are explicitly independent of time t^2 .

²Although the control and state variables are time-dependent, we use the notation x_t and u_t instead of the more common $x(t)$ and $u(t)$ to align with the notation used in Martin and Stahn (2013)

Theorem 1 (Pontryagin's Maximum Principle (PMP)). *Given an admissible state-control trajectory (x_t^*, u_t^*) , $t \in [0, \infty)$, that solves the optimal control problem (8), there exists an absolutely continuous function $\lambda_t : (0, \infty) \rightarrow \mathbb{R}^n$ such that the following conditions are verified:*

- (i) $\dot{x} = f(x_t^*, u_t^*, t)$, $x_0^* = x_0$,
- (ii) $\dot{\lambda} = \rho\lambda_t - H_x(x_t^*, u_t^*, \lambda_t)$,
- (iii) $H(x_t^*, u_t^*, \lambda_t) \geq H(x_t^*, u_t, \lambda_t)$ for each $t \in [0, \infty)$ and for all $u_t \in \mathcal{U}(t)$.
- (iv) Transversality conditions (T.C.)

$$\lim_{t \rightarrow \infty} e^{-\rho t} \lambda_t \geq 0 \quad \text{and} \quad \lim_{t \rightarrow \infty} e^{-\rho t} \lambda_t \cdot x_t^* = 0. \quad (10)$$

Remark 2. *In the particular case that the solution is an interior solution, the maximizing Hamiltonian condition (iii) is satisfied if $\frac{\partial H}{\partial u}(x_t^*, u_t^*, \lambda_t) = 0$.*

To ensure the optimality of a candidate (x_t^*, u_t^*) that satisfies the aforementioned first-order conditions (F.O.C.), we employ *Arrow's Theorem*. For this purpose, the Standard Hamiltonian is defined, where the control function $u_t^* = u_t^*(x_t, \lambda_t)$ is implicitly and uniquely defined by:

$$H^0(x_t, \lambda_t) = \max_{u_t \in \mathcal{U}(t)} H(x_t, u_t, \lambda_t) = \phi(x_t, u_t^*, t) + \lambda(t)f(x_t, u_t^*, t). \quad (11)$$

Theorem 3 (Sufficiency Conditions for Discounted Infinite-Horizon Problems). *Let u_t^* , and the corresponding x_t^* and λ_t , satisfy the PMP necessary conditions for all $t \in [0, \infty)$. Then, the pair (x_t^*, u_t^*) achieves the global maximum of (8) if the Standard Hamiltonian $H^0(x_t, \lambda_t)$ is concave in x_t for each $t \in [0, \infty)$.*

This theorem establishes that concavity of $H^0(x_t, \lambda_t)$ ensures the sufficiency of the necessary conditions for optimality, providing a guarantee that the candidate trajectory (x_t^*, u_t^*) is globally optimal under the given constraints.

Finally, the optimal long-run equilibrium values for the state, control, and co-state variables, denoted as x^e , u^e and λ^{e3} must satisfy the following conditions:

$$\begin{cases} f(x^e, u^e) = 0, \\ \rho\lambda^e - H_x(x^e, u^e, \lambda^e) = 0, \\ H(x^e, u^e, \lambda^e) \geq H(x^e, u, \lambda^e) \quad \forall u \in \mathcal{U}(t). \end{cases} \quad (12)$$

These conditions define the steady-state behavior of the system, ensuring that the equilibrium satisfies the necessary conditions for optimality in the infinite time horizon.

³We shall use $x^e(1)$, $x^e(0)$ and x_e to denote the steady state of the state variable x_t in the Linear Model with full fertilizers, the model described in Martin and Stahn (2013) and the Non-Linear Model, respectively.

4 Modeling groundwater pollution

This section applies the optimal control theory framework outlined in Section 3 to model the joint dynamics of aquifer water levels and quality, and to evaluate their impact on food and water consumption. The analysis integrates the effects of fertilizer use on these systems to derive socially optimal policies.

After defining the problem and specifying the functional forms, Section 4.2 introduces two models, differing in their treatment of food price reductions due to fertilizer use. In Section 4.3, we derive the equilibrium solutions for the Linear model and compare them to those of the Non-Linear model in Section 4.4.

The Non-Linear model is introduced to address the limitations of the Linear model, as discussed in Section 4.2, where fertilizer use is restricted to extreme values—either complete prohibition or full application. In contrast, the Non-Linear model allows for continuous variation in fertilizer use across its full range, thereby aiming to maximize social welfare more effectively.

Farmer decision-making plays a crucial role in determining fertilizer use, influenced by perceived risks and incentives. For example, evidence from (Pan et al., 2020), indicates that farmers reduce fertilizer expenditure in response to profitability risks, while environmental risks have little influence on their decisions. Other factors, such as access to information, financial incentives, social norms, macroeconomic conditions, and environmental awareness, also affect these choices.⁴

Within this framework, social welfare is maximized without explicitly modeling individual agents. Instead, the environmental costs of fertilizer use—primarily related to water purification—are internalized and incorporated into the utility maximization process.

4.1 The models

This study examines the coupled dynamics of aquifer water levels and quality, and their effects on food and water consumption. Aquifer levels depend on crop irrigation, which contributes to recharge at rate b , while fertilizer use introduces contaminants at rate η . Natural pollutant degradation occurs at rate δ . Water extracted for consumption must be treated when polluted, resulting in additional societal costs.

Consumers derive utility from the surplus of food and water consumption and exhibit environmental preferences through the desired aquifer height. When the water level deviates from the optimal benchmark, \bar{h} , social utility decreases. Fertilizer use influences food prices via the cost function $c(\gamma_t)$ defined in (4), with price reductions increasing consumer surplus. The parameter d reflects consumers' willingness to pay for food.

A policy-relevant scenario arises when $\beta < 0$, corresponding to a fertilizer tax. As demonstrated in Proposition 4, fertilizer use becomes suboptimal, since the associated food price increase removes any economic incentive to apply it. This highlights the role of policy interventions in regulating fertilizer use.

The model includes three control variables: food consumption (or production) f_t , measured in mass per units of time, groundwater extraction g_t , measured in units of volume per unit of time; and the pollutant input from fertilizer use γ_t , which is dimensionless. The state variables are the aquifer water height h_t , and the water quality Ψ_t , both dimensionless normalized between 0 and 1. These together form the state vector $x(t) \in \mathbb{R}^2$ while the control vector is $u(t) \in \mathbb{R}^3$.

⁴See Table 3 in Liu et al. (2018) for a review of these factors.

The dynamics of the system are governed by the differential equations for aquifer height and water quality, previously introduced in (2) and (7), respectively, and derived in Section 2.2.

This model builds on the framework established in Martin and Stahn (2013), which introduces surplus functions for water consumption and environmental externalities. Our extension incorporates fertilizer use and its impact on food prices, introducing the pollutant input γ_t directly into the surplus functions, as detailed in Section 4.1.

This modification enables an integrated analysis of the trade-offs between food production and environmental outcomes—specifically, the impact of fertilizer use on aquifer quality. It addresses a key limitation in the original model, which assumes chemical-free agriculture and omits pollution-related effects.

The social utility function

$$U_1(h_t, \Psi_t, f_t, g_t, \gamma_t) = -\frac{1}{2}g_t^2 + g_th_t + (d + D(\gamma_t))f_t - \frac{1}{2}f_t^2 - \frac{1}{2}(h_t - \bar{h})^2 - \frac{1}{2}(1 - \Psi_t)^2, \quad (13)$$

comprises three components:

- **surplus from water consumption:**

$$\sigma(h_t, g_t) = -\frac{1}{2}g_t^2 + g_th_t, \quad (14)$$

- **food consumption surplus:**

$$s(f_t, \gamma_t) = (d + D(\gamma_t))f_t - \frac{1}{2}f_t^2, \text{ where } \begin{cases} D(\gamma_t) = \beta\gamma_t & \textbf{(Linear case)} \\ D(\gamma_t) = \beta\gamma_t^{1/2} & \textbf{(Non-Linear case)} \end{cases}, \quad (15)$$

- **environmental externality:**

$$e(h_t, \Psi_t) = -\frac{1}{2}(h_t - \bar{h})^2 - \frac{1}{2}(1 - \Psi_t)^2. \quad (16)$$

Accordingly, total social utility is given by:

$$U_1(h_t, \Psi_t, f_t, g_t, \gamma_t) = \sigma(h_t, g_t) + s(f_t, \gamma_t) + e(h_t, \Psi_t). \quad (17)$$

The main distinction between our models and those of Martin and Stahn (2013) lies in the inclusion of fertilizer-driven food price reductions through $D(\gamma_t)$ and the integration of a social cost associated with deteriorating water quality. Consequently, our social utility function $U_1(f_t, g_t, \gamma_t, h_t, \Psi_t)$ relates to their formulation $U_0(f_t, g_t, h_t)$ (see (1)) as follows:

$$U_1(h_t, \Psi_t, f_t, g_t, \gamma_t) = U_0(h_t, f_t, g_t) + D(\gamma_t)f_t - \frac{1}{2}(1 - \Psi_t)^2. \quad (18)$$

4.2 The Problem

Based on the theoretical framework established in (8), the problem can be formulated as the following optimal control problem:

$$\left\{ \begin{array}{l} \max_{f_t, g_t, \gamma_t} \int_0^\infty \left[-\frac{1}{2}g_t^2 + g_th_t + (d + D(\gamma_t))f_t - \frac{1}{2}f_t^2 - \frac{1}{2}(h_t - \bar{h})^2 - \frac{1}{2}(1 - \Psi_t)^2 \right] e^{-\rho t} dt \\ \text{subject to: } \begin{cases} \dot{\Psi}_t = \delta(1 - \Psi_t) - \eta f_t \gamma_t, & \Psi_0 = 1, \quad \Psi_t \in [0, 1], \quad \gamma_t \in [0, 1], \\ \dot{h}_t = bf_t - g_t, & h_0 = 1, \quad h_t \in [0, 1], \\ \rho + \delta = 1, & \rho, \delta \in [0, 1], \quad \eta, b \in [0, 1], \end{cases} \end{array} \right. \quad (19)$$

where $D(\gamma_t)$ is given by (15).

The objective is to maximize the present value of social utility subject to dynamic constraints governing the evolution of water quality and aquifer height. The optimal trajectories for groundwater consumption, fertilizer use and food consumption are determined by solving this problem under specific boundary and feasibility conditions. These trajectories reflect the decisions of a central planner seeking to achieve socially optimal outcomes.

The formulation of this problem relies on key assumptions regarding resource sustainability and pollution dynamics. One central assumption is that the sum of the discount factor and the natural degradation rate of pollution equals one ($\rho + \delta = 1$). This condition reflects the idea that future consumption is valued more when natural systems, such as aquifers, have a high capacity to purify water. This aligns with the notion of the "tragedy of the commons" (Hardin, 1968), wherein over-exploitation occurs when natural resources are unable to regenerate fast enough. If the discount rate ρ approaches its upper bound, the model predicts a decline in groundwater consumption toward zero, indicating low long-term sustainability. Additionally, empirical evidence from Corral-Verdugo, Frias-Armenta, Pérez-Urias, Orduña-Cabrera, and Espinoza-Gallego (2002) suggests that perceptions of collective behavior influence individual water consumption, with consumers being less inclined to conserve resources if they believe others are wasting them.

The model also incorporates a sustainability constraint that requires the resource growth rate b —representing irrigation inflows—to exceed the social discount rate ρ ($b > \rho$). This condition, which builds on the findings of Manzoor, Aseev, Rovenskaya, and Muhammad (2014), ensures that the system can maintain long-term balance between extraction and replenishment.

Pollution dynamics are modeled to capture both benefits and costs of fertilizer use. While fertilizers improve food production, they also introduce pollutants into the aquifer. In the Linear Model, these benefits are captured through a linear discount effect on food prices, whereas the Non-Linear Model assumes diminishing returns, consistent with studies such as Brock et al. (2014). The environmental costs, primarily related to water purification, are incorporated through convex damage functions in both cases.

For the Linear Model, the current-value Hamiltonian takes the following form:

$$\begin{aligned} H_1(h_t, \Psi_t, f_t, g_t, \gamma_t, \lambda_t, \mu_t) = & -\frac{1}{2}g_t^2 + g_th_t + (d + \beta\gamma_t)f_t - \frac{1}{2}f_t^2 - \frac{1}{2}(h_t - \bar{h})^2 - \frac{1}{2}(1 - \Psi_t)^2 \\ & + \lambda_t[\delta(1 - \Psi_t) - \eta f_t \gamma_t] + \mu_t[bf_t - g_t]. \end{aligned} \quad (20)$$

This expression captures the dynamic interactions among state and control variables—including aquifer height, water quality, food production, groundwater extraction, and fertilizer use—while balancing productivity gains from fertilizer use against the social costs of groundwater pollution. Since the Hamiltonian is linear in the fertilizer input γ_t , the

optimal path for γ_t follows a bang-bang control policy. The switching rule depends on the relationship between the price-discount parameter β , the pollution factor η , and the shadow price of water quality, λ_t :

$$\gamma_t^* = \begin{cases} 1 & \text{if } \frac{\beta}{\eta} > \lambda_t \\ - & \text{if } \frac{\beta}{\eta} = \lambda_t \\ 0 & \text{if } \frac{\beta}{\eta} < \lambda_t. \end{cases} \quad (21)$$

When $\gamma_t^* = 0$, the optimal paths coincide with those of the baseline model by Martin and Stahn (2013), providing a baseline for comparison against fertilizer-based scenarios.

Alternatively, the Non-Linear Model allows for intermediate levels of fertilizer application. Under certain parameter configurations, fertilizer use declines to zero when the price reduction effect, β , diminishes (see (C.8)). The equilibrium points (C.4) in this model are computed numerically using the Newton-Raphson method (Yang, 2017), which determines the steady-state fertilizer input γ_e within the admissible range $[0, 1]$. To assess local stability, the system derived from the Maximum Principle is linearized around the equilibrium using Hartman's theorem (Hartman & Wintner, 1953).

The current-value Hamiltonian for the Non-Linear Model is given by:

$$H(h_t, \Psi_t, f_t, g_t, \gamma_t, \lambda_t, \mu_t) = -\frac{1}{2}g_t^2 + g_th_t + (d + \beta\gamma_t^{\frac{1}{2}})f_t - \frac{1}{2}f_t^2 - \frac{1}{2}(h_t - \bar{h})^2 - \frac{1}{2}(1 - \Psi_t)^2 + \lambda_t[\delta(1 - \Psi_t) - \eta f_t \gamma_t] + \mu_t[b f_t - g_t]. \quad (22)$$

Using the respective Hamiltonians, the optimal paths are derived and validated against the transversality conditions presented in the Appendix 8. These trajectories offer insights into the dynamic evolution of groundwater use, food production, and pollution control. Furthermore, both models satisfy Arrow's sufficiency conditions: their Hamiltonians are concave in the relevant state variables, guaranteeing the global optimality of the solutions under both linear and non-linear representations of fertilizer-induced food price effects.

4.3 Analysis of Equilibria and Parameters in the Linear Model

The linearity of the Hamiltonian (20) in the fertilizer input yields two distinct policy regimes, determined by the shadow price of water quality, λ_t , as compared to a threshold defined by the ratio $\frac{\beta}{\eta}$. If the shadow price of quality water, λ_t , falls below $\frac{\beta}{\eta}$, social utility is maximized by forgoing fertilizer use. Conversely, when λ_t exceeds this threshold, setting $\gamma_t = 1$ becomes optimal.

We analyze the parametric constraints governing these regimes and offer a comparative analysis of equilibria under full versus zero fertilizer use, extending the framework of Martin and Stahn.

We begin by establishing Proposition 4, which demonstrates that when fertilizer use leads to higher food prices ($\beta < 0$), the optimal level of fertilizer application is zero ($\gamma_t^* = 0$). In that case, water quality remains at its maximum level, while the optimal paths for food consumption, groundwater extraction, and aquifer height match the trajectories derived in the baseline model.

Proposition 4. *If $\beta < 0$, the optimal level of fertilizer use in the problem (19) with $D(\gamma_t) = \beta\gamma_t$ is $\gamma_t^* = 0$. Additionally, the optimal path for water quality is $\psi_t^* = 1$ while the optimal paths for food, groundwater consumption and aquifer height, (h_t^*, f_t^*, g_t^*) align with those in Martin and Stahn (2013).*

The proof and corresponding expressions for (f_t^*, g_t^*, h_t^*) are provided in Appendix A.

The conditions that lead to the optimal control $\gamma_t^* = 1$ are outlined in Proposition 5. This analysis focuses on stable intertemporal solutions, which are critical for resource management and long-term policy planning. Stability is ensured by selecting paths associated with negative eigenvalues, which prevent significant deviations in equilibrium due to small perturbations. Focusing the analysis on stable paths guarantees that policy implementation remains consistent over time.

When $\beta > 0$, the optimality of fertilizer use depends on the system's stability and parametric constraints. Proposition 5 characterizes these conditions.

Proposition 5. *Let $\beta > 0$ and suppose $\frac{\bar{h}}{2-\delta} < \min\{\frac{\eta^2+\delta(1-b(\beta+d))}{\eta^2+\delta(1+b^2)}, \frac{\eta^2+\delta-\eta(\beta+d)}{\eta b}\}$. Then, if either $\beta > \eta$, or $\beta < \eta$ and $f^e(0) = \frac{b\bar{h}}{2-\delta} + d \leq \frac{\beta\delta}{\eta^2}$, the stable intertemporal efficient paths for the problem (19) with $D(\gamma_t) = \beta\gamma_t$ are given by (B.6) with $\gamma_t^* = 1$.*

The proof of Proposition 5 is detailed in Appendix B.

The case $\beta > \eta$ in Proposition 5 implies that when the reduction in food costs due to fertilizer use exceeds the marginal environmental cost of pollution –represented in the model by the pollution coefficient η – setting $\gamma_t^* = 1$ becomes optimal. Conversely, if the environmental damage outweighs the cost reduction from fertilizer use ($\beta < \eta$), maximum application becomes optimal only when the combined value of water storage ($\mu^e(1) = \mu^e(0) = \frac{\bar{h}}{\rho+1}$) and food demand, d , does not exceed the benefits from fertilizer-driven food price reductions. When this condition is satisfied, the system can sustain maximum fertilizer use without compromising the resource. As evidenced in Table 1 below, when β is relatively low the optimal policy is to use no fertilizer, whereas for higher values full fertilizer use is optimal. This balance highlights the role of parametric interactions in determining optimal resource management strategies.

Scenario	β	h_e	Ψ_e	γ_e	μ_e	λ_e	g_e	f_e	$U^e(1)$	$U^e(0)$
Full	0.3	0.678	0.289	1	0.112	0.711	0.566	0.809	0.541	
Zero	0.3	0.867		0	0.112		0.755	1.078		0.589
Full	0.4	0.719	0.237	1	0.112	0.763	0.608	0.868	0.621	
Zero	0.4	0.867		0	0.112		0.755	1.078		0.589
Full	0.5	0.761	0.185	1	0.112	0.815	0.649	0.927	0.708	
Zero	0.5	0.867		0	0.112		0.755	1.078		0.589

Table 1: Comparison of equilibrium outcomes under full and zero fertilizer use for different values of β . Parameters: $\eta = 0.8, \rho = 0.09, d = 1, \bar{h} = 0.122, b = 0.7$

A comparison of equilibria with and without fertilizer use further highlights the non-linear dependencies between key parameters and optimal policy outcomes. The Linear Model equilibria can be expressed in relation to the benchmark model proposed by Martin and Stahn as follows:

$$\begin{aligned}
\mu^e(1) &= \frac{\bar{h}}{\rho + 1} = \mu^e(0) \\
\lambda^e(1) &= \frac{\eta}{(\eta^2 + \delta)}(f^e(0) + \beta) \\
f^e(1) &= (f^e(0) + \beta) \frac{\delta}{(\eta^2 + \delta)} > f^e(0) = d + \frac{b\bar{h}}{1 + \rho} \iff f^e(0) < \frac{\beta\delta}{\eta^2} \\
\psi^e(1) &= 1 - \lambda^e(1) = 1 - \frac{\eta}{(\eta^2 + \delta)}(f^e(0) + \beta) \\
g^e(1) &= bf^e(1) > bf^e(0) = g^e(0) \iff f^e(0) < \frac{\beta\delta}{\eta^2} \\
h^e(1) &= \mu^e(1) + g^e(1) > \mu^e(0) + g^e(0) = h^e(0) \iff f^e(0) < \frac{\beta\delta}{\eta^2}
\end{aligned} \tag{23}$$

Here, the subscript " $e(0)$ " refers to the equilibrium values under the benchmark model without fertilizer use ($\gamma_t^* = 0$), while " $e(1)$ " denotes the equilibrium values under full fertilizer use ($\gamma_t^* = 1$).

These relationships are summarized in the following proposition:

Proposition 6. *For the problem (19) with $D(\gamma_t) = \beta\gamma_t$, if $f^e(0) < \frac{\beta\delta}{\eta^2}$, the equilibrium values for food consumption, groundwater extraction, and aquifer height with full fertilizer use ($\gamma_t^* = 1$) are strictly greater than those obtained without fertilizer use ($\gamma_t^* = 0$). Conversely, if $f^e(0) \geq \frac{\beta\delta}{\eta^2}$, no such improvement is observed in equilibrium values.*

The relationships in (23) highlight the strong dependence of social utility on the interplay between price discounts (β), pollutant generation (η), and natural degradation (δ). Utility will exceed that of the Martin and Stahn scenario only if price discounts and natural degradation effectively offset fertilizer-induced pollution.

To further illustrate these dynamics, we present two examples. Figure 1 satisfies the condition $f^e(0) \geq \frac{\beta\delta}{\eta^2}$, while the case shown in Figure 2 does not. Both figures display the optimal trajectories for the Linear Model with and without fertilizer application. Each scenario's corresponding equilibrium values are also shown

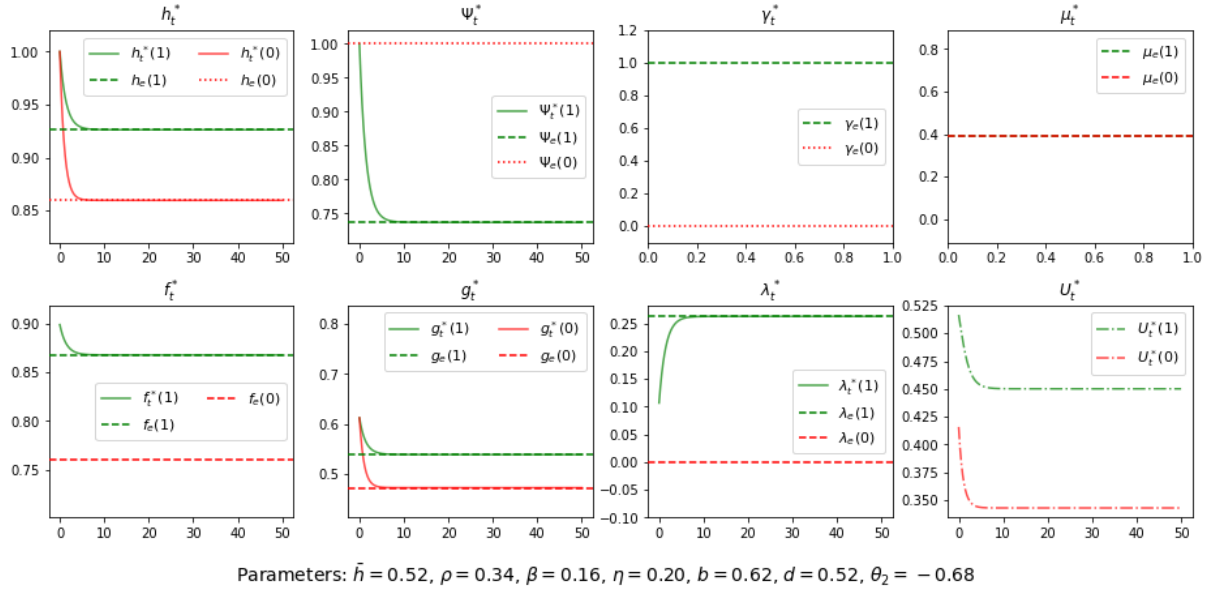


Figure 1: In this scenario, where $f^e(0) \approx 0.761 < \frac{\beta\delta}{\eta^2} \approx 2.64$, full fertilizer application leads to improved equilibrium values, indicating that fertilizer-induced food price discounts, together with the system's natural degradation capacity, effectively mitigate pollutant generation.

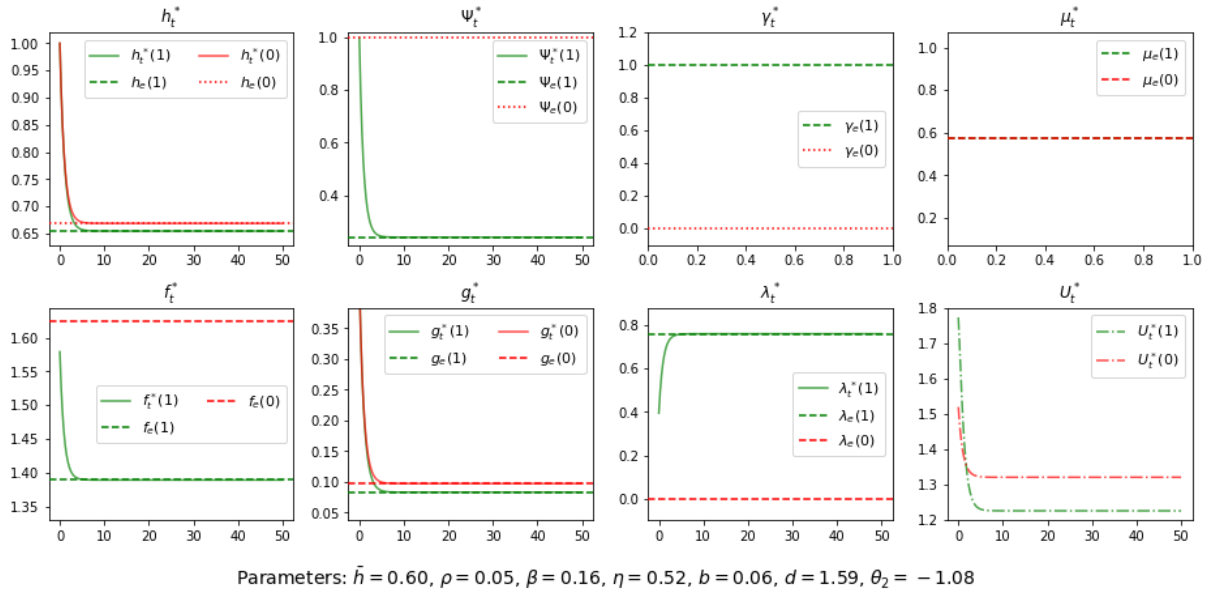


Figure 2: In this case, we find that $f^e(0) \approx 1.625$, which is greater than $\frac{\beta\delta}{\eta^2} \approx 0.562$. Full fertilizer application does not improve equilibrium outcomes, indicating that the benefits of reduced food prices are insufficient to offset the negative environmental impacts of pollution.

The shadow price $\lambda^e(1)$, associated with water quality under fertilizer use, reflects the interplay between pollution generation, natural degradation, and food production. This balance is quantified by the ratio $\frac{\eta}{\eta^2 + \delta}$. It increases with pollution (η) and decreases with stronger natural degradation (δ), thus capturing the environment's ability to offset contamination.

This trade-off has clear policy implications: robust natural degradation (δ) mitigates pollution and lowers $\lambda^e(1)$. However, if pollution from fertilizers (η) far exceeds δ , stringent regulatory measures may be necessary. In particular, when $\beta < 0$, fertilizer use becomes counterproductive: since $f^e(0) > \frac{\beta\delta}{\eta^2}$, it follows that $f^e(1) < f^e(0)$, and utility is maximized without fertilizer.

In essence, $\lambda^e(1)$ represents the marginal social cost of maintaining water quality under fertilizer use, balancing agricultural benefits against ecological damage. A high $\lambda^e(1)$ signals that pollution costs outweigh food productivity gains, justifying stricter regulations or alternative agricultural practices. Conversely, when natural degradation (δ) effectively mitigates contamination, the resulting environmental damage is lower, allowing for more flexible management strategies. Ultimately, the value of $\lambda^e(1)$ reflects society's trade-off between economic growth and environmental sustainability, guiding policy decisions on fertilizer use and water resource management.

We now turn to the role of fertilizer-induced food price reductions in shaping system dynamics, depending on the regeneration capacity of the ecosystem and the extent of aquifer pollution. The functions $f(\eta) := \frac{\eta}{\eta^2 + \delta}$ and $\mathbf{h}(\eta) := \frac{\delta}{\delta + \eta^2}$ (illustrated in Figures 3 and 4, respectively) provide further insight into the impact of pollution intensity and degradation capacity on equilibrium outcomes. Specifically, $f(\eta)$ has the property that

$$f(\eta) < 1 \iff \delta > \eta - \eta^2, \quad (24)$$

increasing when $\eta \in (0, \sqrt{\delta})$ and decreasing when $\eta > \sqrt{\delta}$. It achieves its maximum at $\eta = \sqrt{\delta}$, with $f(\sqrt{\delta}) = \frac{1}{2\sqrt{\delta}}$. If $\delta > 0.25$, then $f(\eta) < 1$ for all $\eta \in [0, 1]$. Conversely, if $0 < \delta < 0.25$, there exists a range of η for which $f(\eta) > 1$.

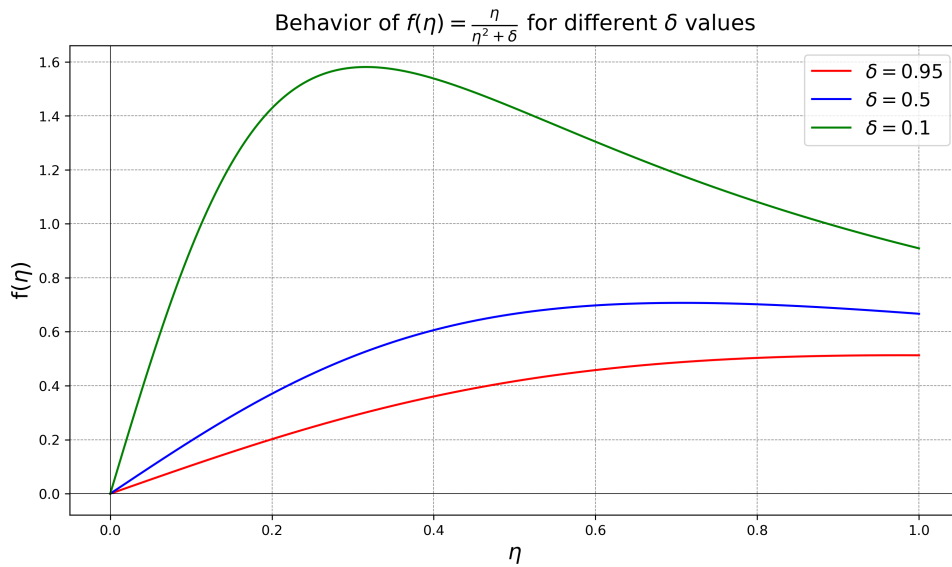


Figure 3: If $\delta > 0.25$, then $f(\eta) < 1$ for all $\eta \in [0, 1]$ while, if $0 < \delta < 0.25$, $f(\eta) > 1 \forall \eta \in [\frac{1-\sqrt{1-4\delta}}{2}, \frac{1+\sqrt{1-4\delta}}{2}]$

Consequently, if the rate of natural degradation is high, the system can compensate for increased pollution by maintaining or improving water quality, thus lowering $\lambda^e(1)$. A lower shadow price indicates that the system is better equipped to absorb or neutralize additional pollutant loads without compromising water quality. Conversely, when natural degradation is low, it becomes more difficult for the system to counteract rising pollutant levels effectively.

The function $\mathbf{h}(\eta) = \frac{\delta}{\delta + \eta^2}$ captures how the system's capacity to degrade pollution shapes the equilibrium outcomes of food consumption, groundwater extraction, and aquifer height. Although $\mathbf{h}(\eta)$ does not directly represent water quality, it plays a crucial role in the system's dynamic behavior.

At $\eta = 0$, $\mathbf{h}(0) = 1$, suggesting that, in the absence of pollution, price discounts (β) have a stronger effect on food production. At low values of η , price discounts therefore act as an effective incentive for food production. However, as η increases, $\mathbf{h}(\eta)$ decreases, indicating that higher pollution levels reduce food production efficiency and weaken the incentive to consume water. This leads to lower water extraction and a decline in aquifer height.

When $\mathbf{h}(\eta)$ is high (e.g., due to strong natural degradation, δ), the system is able to mitigate the effects of pollution more effectively, allowing higher levels of food and water consumption. Conversely, when $\mathbf{h}(\eta)$ is low—either because natural degradation is weak or pollutant input is high—pollution accumulates more rapidly. As a result, food and water consumption must decrease to preserve long-term resource availability.

An important factor is how the discount on food prices, β , interacts with these dynamics. When η is small, $\mathbf{h}(\eta) \approx 1$, making price discounts more effective in incentivizing increased food production. However, as pollution intensifies, this incentive weakens, leading to diminished production efficiency and reduced equilibrium resource levels.

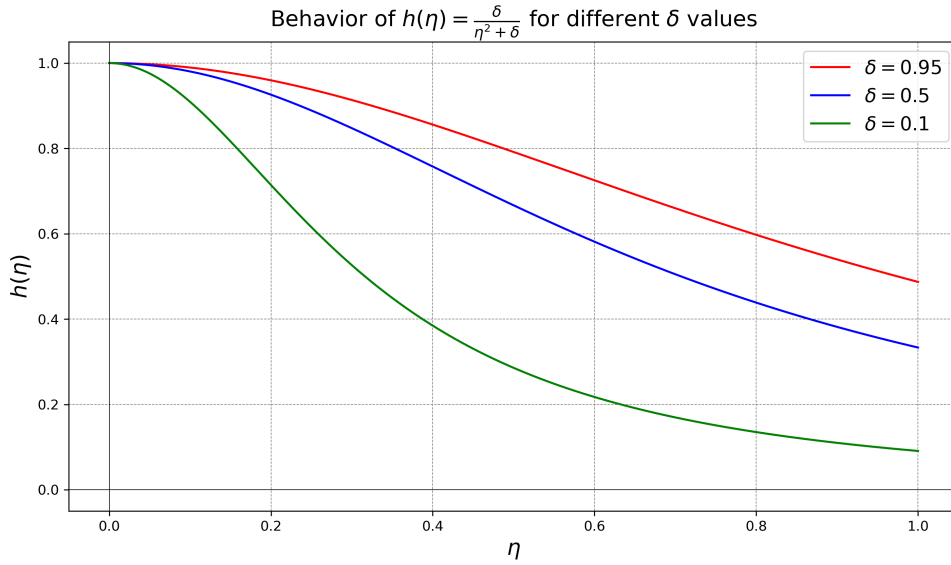


Figure 4

This analysis illustrates how pollution input η and the natural degradation rate δ affect the equilibrium levels of food consumption, groundwater extraction, and aquifer height. When δ is relatively high or η is low, the equilibrium outcomes under fertilizer use improve relative to those without fertilizer, as the system offsets pollution more effectively. Conversely, low δ and high η reduce the beneficial effects of fertilizer-induced price discounts, potentially leading to lower equilibrium levels of food and water use.

The utility derived from full fertilizer use depends on the balance of these parameters, represented by $\frac{\beta\delta}{\eta^2}$. A higher degradation rate δ amplifies the positive effect of β on food consumption and water use, leading to higher equilibrium utility. In contrast, when pollution generation (through large η) dominates, the environmental costs outweigh the benefits, resulting in lower social utility.

When natural purification capacity is strong, full fertilizer use can be sustained with limited environmental risk. However, increasing pollution—often driven by climate change—may erode this resilience by overwhelming the system’s capacity to absorb contaminants. Evidence from studies on public perception of environmental issues (Anderson, Romani, Phillips, Wentzel, & Tlabela, 2007; Tran, Euan, & Isla, 2002) suggests that public awareness can guide policy strategies to mitigate pollution and manage water resources sustainably.

Furthermore, climate change exacerbates water pollution by accelerating pollutants desorption, weakening the system’s capacity to preserve water quality. This dynamic is underscored by the United Nations:

“Water and climate change are inextricably linked. Extreme weather events are making water more scarce, more unpredictable, more polluted or all three. These impacts throughout the water cycle threaten sustainable development, biodiversity, and people’s access to water and sanitation.” (United Nations, 2024).

4.4 Analysis of Equilibria and Parameters in the Non-Linear Model

This section analyzes the equilibrium outcomes under a concave price discount model induced by fertilizer use, capturing diminishing returns. We present a key proposition characterizing the equilibria and comparing them to both the fertilizer-free benchmark model and the linear model with full fertilizer application.

Proposition 7 (Optimal equilibrium under concave fertilizer model). *Consider the concave impact of fertilizer use on food prices as described in the control problem (19) with $D(\gamma_t) = \beta\gamma_t^{1/2}$. Suppose that $0 < \beta \leq 2\eta$, $1 - \rho > \frac{\beta^4}{16\eta^2}$, $\frac{\bar{h}}{\rho+1} \leq 1 - \frac{b\beta}{2}$, along with the following parametric constraint:*

$$\frac{\beta(1-\rho)}{2\eta^2} - \frac{\beta}{2} \leq b\frac{\bar{h}}{\rho+1} + d \leq \min \left\{ \frac{4\eta(1-\rho)}{\beta^2} - \frac{\beta^2}{4\eta}, \frac{1}{b} \left(1 - \frac{\bar{h}}{\rho+1} \right) - \frac{\beta}{2} \right\}. \quad (25)$$

Then, a unique equilibrium vector $(h_e, \Psi_e, f_e, g_e, \gamma_e, \lambda_e, \mu_e)$ exists, satisfying:

$$\begin{aligned} \mu_e &= \frac{\bar{h}}{\rho+1}, \quad \lambda_e = \frac{\beta}{2\eta}\gamma_e^{-1/2}, \quad \Psi_e = 1 - \lambda_e, \quad \gamma_e = \frac{\beta^2}{4\eta^2\lambda_e^2}, \\ h_e &= bd + b\frac{\beta}{2}\gamma_e^{1/2} + (1+b^2)\mu_e, \quad f_e = d + \frac{\beta^2}{4\eta\lambda_e} + b\mu_e, \quad g_e = h_e - \mu_e. \end{aligned} \quad (26)$$

where $\frac{\beta^2}{4\eta^2} \leq \gamma_e \leq 1$, and $\Psi_e, \lambda_e \in [0, 1]$. Moreover, the following properties hold:

1. If $\beta > 0$, the equilibrium values h_e , f_e , and g_e exceed those in the Linear Model without fertilizers ($\gamma_t^* = 0$).
2. If $\beta < \eta$, the equilibrium values h_e , g_e , and f_e also exceed those of the Linear Model with full fertilizer use ($\gamma_t^* = 1$).
3. System stability is ensured by the presence of two negative eigenvalues, which guarantee the existence of stable trajectories near the equilibrium. The approximate optimal paths, derived by linearizing the system at the steady state, are given in (C.6).

4. As $\beta \rightarrow 0$, fertilizer use vanishes, and the solution converge to those in Martin and Stahn (2013).

Most of the proof is given in Appendix refappendix D; here, we focus on the equilibrium comparisons.

Proof. Let $\beta > 0$. Then,

$$\begin{aligned}\mu_e &= \frac{\bar{h}}{\rho + 1} = \mu^e(0), \\ f_e &= d + b\mu_e + \frac{\beta^2}{4\eta\lambda_e} = f^e(0) + \frac{\beta^2}{4\eta\lambda_e} > f^e(0), \\ h_e &= bd + (1 + b^2)\mu_e + b\frac{\beta}{2}\gamma_e^{1/2} = h^e(0) + b\frac{\beta}{2}\gamma_e^{1/2} > h^e(0), \\ g_e &= h_e - \mu_e = g^e(0) + b\frac{\beta}{2}\gamma_e^{1/2} > g^e(0).\end{aligned}\tag{27}$$

Now suppose $\beta < \eta$. Using (23) and (27) yields

$$\begin{aligned}\mu_e &= \mu^e(1) = \frac{\bar{h}}{\rho + 1}, \\ f_e &= d + b\mu_e + \frac{\beta^2}{4\eta\lambda_e} = f^e(0) + \frac{\beta^2}{4\eta\lambda_e} = \frac{\eta^2 + \delta}{\delta}f^e(1) - \beta + \frac{\beta^2}{4\eta\lambda_e} > f^e(1) + \eta - \beta > f^e(1), \\ h_e &= bf_e + \mu_e > bf^e(1) + \mu^e(1) = h^e(1), \\ g_e &= h_e - \mu_e > h^e(1) - \mu^e(1) = g^e(1),\end{aligned}\tag{28}$$

The inequality for f_e holds because $\frac{\eta^2 + \delta}{\delta} > 1$ and, since $\gamma_e \in \left[\frac{\beta^2}{4\eta^2}, 1\right]$, it follows that implies $\lambda_e = \frac{\beta}{2\eta}\gamma_e^{-1/2} \in \left[\frac{\beta}{2\eta}, \frac{\beta^2}{4\eta^2}\right]$, which ensures that $\frac{\beta^2}{4\eta\lambda_e} > \eta$. \square

5 Numerical results

This section presents numerical simulation results, initially using the parameter set from Martin and Stahn (2013), comparing pollution models with the benchmark model without fertilizer use.

The baseline parameters are $b = 0.16$, $d = 2$ and $\rho = 0.05$. It is important to note that any modifications to the values of η and β must be implemented consistently, assuming all other parameters remain constant (*ceteris paribus*).

The first objective of this study is to investigate the impact of the price discount parameter β on social utility maximization and the equilibrium outcomes of the models. Subsequently, the Non-Linear Model is used to analyze the influence of both β and the pollutant generation parameter η on the optimal choice of fertilizer use. This additional analysis is particularly pertinent because, in the Linear Model with $\gamma_t^* = 1$, fertilizer use is fixed at its maximum level, which prevents assessing the effect of varying pollution levels.

Assessing the effect of β on social utility is critical, as this parameter may serve as a policy instrument to mitigate water pollution. For example, reducing the price discount from fertilizer use could be achieved through measures that internalize its environmental costs, such as taxes (Uri, 1997; Weersink, Livernois, Shogren, & Shortle, 1998). Moreover,

empirical evidence (Guo, Li, Cao, Cao, & Huang, 2021) suggests that agricultural subsidies can effectively reduce fertilizer use—and, consequently, pollution.

In Section 5.1, we summarize the effects of varying β in the Linear Model by comparing the resulting social utility with that of the fertilizer-free benchmark. We also analyze the optimal paths for β values that yield maximum and zero water quality, and we examine the impact of food rebates on aquifer height.

In Section 5.2, a similar analysis is performed for the Non-Linear Model, incorporating different levels of fertilizer-induced pollution. These results are compared with the simulated food rebate scenario and the outcomes of the Linear Model. Finally, Section 5.3 summarizes the findings and discusses the implications of the models for policymaking.

5.1 Simulation Results for the Linear Model

Simulation 1. Table 2 presents the results of simulations that evaluate how varying food rebate values (β) affect the Linear Model, assuming a fixed level of pollution from fertilizer use.

Scenario	β	h_e	ψ_e	γ_e	μ_e	λ_e	g_e	f_e	$U^e(1)$	$U^e(0)$
Full	-2.076	0.476	1.000	1	0.476	0.000	0.000	0.000	-0.000	
Zero	-2.076	0.808		0	0.476		0.332	2.076		2.163
Full	-1.913	0.500	0.953	1	0.476	0.047	0.024	0.149	0.012	
Zero	-1.913	0.808		0	0.476		0.332	2.076		2.163
Full	0.000	0.780	0.401	1	0.476	0.599	0.303	1.897	1.967	
Zero	0.000	0.808		0	0.476		0.332	2.076		2.163
Full	1.000	0.926	0.113	1	0.476	0.887	0.450	2.810	4.313	
Zero	1.000	0.808		0	0.476		0.332	2.076		2.163
Full	1.391	0.983	0.000	1	0.476	1.000	0.507	3.167	5.476	
Zero	1.391	0.808		0	0.476		0.332	2.076		2.163

Table 2: Equilibria for different values of β in the Linear Model with low η . Parameters: $b = 0.16$, $d = 2$, $\eta = 0.3$, $\rho = 0.05$. and $\bar{h} = 0.5$

The impact of β on water quality and social utility. To achieve the highest possible water quality under fertilizer use, a sufficiently negative food price discount β would be required. For instance, at $\beta = -2.076$, water quality reaches its upper bound ($\psi_e = 1$), but the associated social utility under full fertilizer use is slightly negative ($U^e(1) \approx -0.00028$), and thus remains well below the benchmark utility without fertilizers. Further reductions in β lead to infeasible equilibria, as key state variables such as ψ_t exceed their admissible bounds. Therefore, decreasing β is not a viable option within the model’s constraints.

As discussed in Section 4.3, when β is negative, the socially optimal decision is to avoid fertilizer use entirely ($\gamma_t^* = 0$), as this policy yields higher utility than applying fertilizers.

Table 2 shows that increasing food price discounts (β) raises both food consumption (f_e) and groundwater extraction (g_e), resulting in higher social utility ($U^e(1)$). These improvements occur despite the deterioration in water quality (ψ_e), illustrating the trade-off between productivity gains and environmental costs. The results underscore how lower food prices incentivize greater resource use, especially when future environmental damages are discounted at the relatively low rate $\rho = 0.05$ —a value adopted from Martin and Stahn

(2013) that reflects strong aquifer regeneration. This low discount rate supports a more patient societal perspective, where long-term considerations weigh heavily in maximizing social welfare.

The selection of an appropriate discount factor for environmental decisions and inter-generational equity has been widely debated for decades (Carson & Tran, 2009; Polasky & Dampha, 2021). Given its critical influence on outcomes, this choice must be made carefully. In the present framework, the discount rate directly corresponds to the aquifer’s natural degradation rate ($\rho + \delta = 1$).

Impact of β on the socially desirable aquifer height. Under the parameters $b = 0.16$, $d = 2$, $\eta = 0.3$ and $\rho = 0.05$, achieving the socially desirable aquifer height ($\bar{h} = 0.5$) through full fertilizer use requires a specific discount value, $\beta^* = -1.9133$. As shown in Table 2, this choice yields an equilibrium where $h_e = \bar{h}$. Deviating from this value alters the outcome:

- A discount lower than β^* leads, in equilibrium, to reduced food production, ground-water extraction, and aquifer level relative to the target \bar{h} .
- A discount above β^* results in excess water availability and over-incentivization of food production, as the equilibrium aquifer level exceeds \bar{h} .

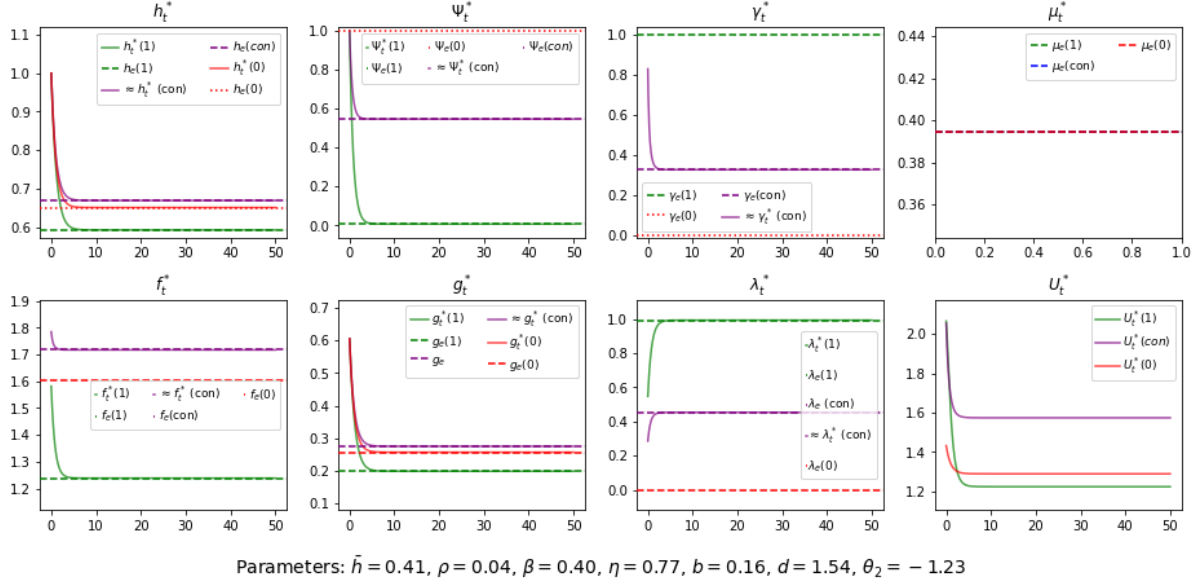
Furthermore, simulations in Table 3 and Figure 5 illustrate that increasing η —the rate of pollution generation—significantly alters the equilibrium outcomes. As environmental damage from fertilizer-induced contamination intensifies, a greater food price discount is required to offset its marginal social cost and validate maximum fertilizer application. This finding highlights the strong sensitivity of the optimal fertilizer policy to the parameter η . However, this compensation has limits: for values of β above approximately 0.435, the model yields infeasible equilibria, as water quality (ψ_e) becomes negative and thus infeasible.

Scenario	β	h_e	ψ_e	γ_e	μ_e	λ_e	g_e	f_e	$U^e(1)$	$U^e(0)$
Total	0.000	0.676	0.214	1	0.467	0.786	0.209	1.044	0.816	
Zero	0.000	0.786		0	0.467		0.319	1.593		1.279
Total	0.100	0.689	0.165	1	0.467	0.835	0.222	1.109	0.921	
Zero	0.100	0.786		0	0.467		0.319	1.593		1.279
Total	0.200	0.702	0.116	1	0.467	0.884	0.235	1.175	1.033	
Zero	0.200	0.786		0	0.467		0.319	1.593		1.279
Total	0.300	0.715	0.067	1	0.467	0.933	0.248	1.240	1.151	
Zero	0.300	0.786		0	0.467		0.319	1.593		1.279
Total	0.400	0.728	0.017	1	0.467	0.983	0.261	1.306	1.276	
Zero	0.400	0.786		0	0.467		0.319	1.593		1.279
Total	0.435	0.733	0.000	1	0.467	1.000	0.261	1.328	1.321	
Zero	0.435	0.786		0	0.467		0.319	1.593		1.279

Table 3: Equilibria for different values of β in the Linear Model with high η . Parameters: $\eta = 0.7$, $\rho = 0.07$, $d = 1.5$, $\bar{h} = 0.5$, $b = 0.2$

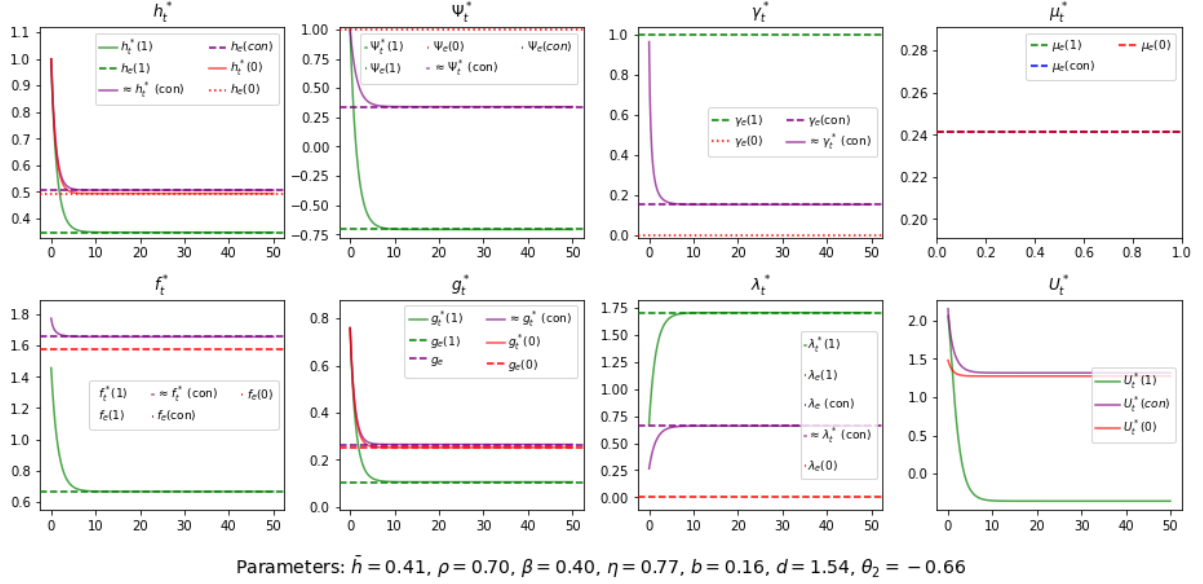
It is worth noting that the parameter values used in Table 3 differ slightly from those in the reference model, as they were adjusted to ensure the feasibility of the equilibria. Nonetheless, the main driver behind the observed shifts in outcomes is the increase in η .

Figure 5: Simulated optimal paths for the three models with $\bar{h} = 0.41$, $\rho = 0.04$, $\beta = 0.4$, $\eta = 0.77$, $b = 0.16$, and $d = 1.54$. A high η significantly impacts the optimal policy, as large food discounts no longer support full fertilizer use and negatively affect water purity. Increasing η raises the critical β .



As illustrated in Figure 5, high levels of fertilizer-induced pollution reduce the effectiveness of food price discounts as an incentive for fertilizer use. In such contexts, full fertilizer application ceases to be optimal. Instead, society would benefit more from either avoiding fertilizers entirely, as in the linear model, or adopting intermediate fertilizer levels that yield better utility outcomes, as captured by the non-linear model. Moreover, additional simulations (see Figure 6) reveal that as the natural absorption capacity diminishes (i.e., when ρ increases and thus $\delta = 1 - \rho$ declines), the zero-fertilizer option becomes relatively more advantageous. This underscores the role of environmental resilience in determining the desirability of fertilizer use and highlights the importance of incorporating natural degradation dynamics into policy design.

Figure 6: Simulated optimal paths for the three models with $\bar{h} = 0.41$, $\rho = 0.70$, $\beta = 0.4$, $\eta = 0.77$, $b = 0.16$, and $d = 1.54$. A lower δ significantly weakens the relative performance of fertilizer-intensive strategies. As δ increases, the environmental cost of fertilizers declines, improving the utility associated with their use.



5.2 Simulation results in the Non-Linear model

Simulation 2. In the context of the Non-Linear Model, we analyze the impact of varying values of the food rebate, β , given a fixed pollution level from fertilizer use, $\eta = 0.3$ (see Table 4).

Scenario	β	h_e	ψ_e	γ_e	μ_e	λ_e	g_e	f_e	$U^e(0)$	U_e
Concave	0.000	0.808	0.999	0.001	0.476	0.001	0.332	2.076		2.163
Zero	0.000	0.808		0.000	0.476		0.332	2.076	2.163	
Concave	0.100	0.813	0.736	0.397	0.476	0.264	0.337	2.108		2.260
Zero	0.100	0.808		0.000	0.476		0.332	2.076	2.163	
Concave	0.200	0.821	0.577	0.621	0.476	0.423	0.345	2.155		2.410
Zero	0.200	0.808		0.000	0.476		0.332	2.076	2.163	
Concave	0.300	0.830	0.441	0.801	0.476	0.559	0.354	2.210		2.592
Zero	0.300	0.808		0.000	0.476		0.332	2.076	2.163	

Table 4: Equilibria for different values of β in the Non-Linear Model. Parameters: $\eta = 0.3$, $\rho = 0.05$, $d = 2$, $\bar{h} = 0.5$, $b = 0.16$.

The impact of β on fertilizers use. Increasing the food rebate encourages greater fertilizers use in food production. This reduces water quality while raising the aquifer level due to higher food production.

It is worth noting that the equilibrium values of fertilizer use remain well below the maximum permissible level. Even when water quality is significantly degraded, the model yields moderate fertilizer application. This reflects a societal preference for more restrained agricultural practices.

The impact of β on quality water level and social utility. While high food

rebates negatively affect long-term water quality, lower rebates contribute positively to its preservation.

Broadly speaking, compared to the fertilizer-free equilibrium, a higher food rebate β leads to increased food production and higher water extraction. This is because lower food prices enhance consumer surplus, similarly to what is observed in the Linear Model.

When β approaches zero, the long-term utility becomes comparable to the no-fertilizer benchmark. In this scenario, aquifer height remains high, water quality approaches its maximum, and fertilizer use is negligible.

Unlike in the Linear Model, negative food discounts are not needed to discourage fertilizer use. Simply keeping rebates close to zero is enough to preserve water quality. In practical terms, this could be achieved narrowing the cost gap between organic and conventional production, for instance through technological improvements.

Simulation 3. We now analyze how variations in pollutant levels, η , affect the Non-Linear model outcomes, holding the food rebate fixed at $\beta = 1$ (see Table 5).

Scenario	η	h_e	ψ_e	γ_e	μ_e	λ_e	g_e	f_e	$U^e(0)$	U^e
Concave	0.650	0.870	0.001	0.593	0.476	0.999	0.394	2.461		3.487
Zero	0.650	0.808		0.000	0.476		0.332	2.076	2.163	
Concave	0.700	0.867	0.028	0.540	0.476	0.972	0.391	2.444		3.420
Zero	0.700	0.808		0.000	0.476		0.332	2.076	2.163	
Concave	0.800	0.862	0.074	0.456	0.476	0.926	0.386	2.414		3.308
Zero	0.800	0.808		0.000	0.476		0.332	2.076	2.163	
Concave	0.900	0.858	0.113	0.392	0.476	0.887	0.382	2.389		3.217
Zero	0.900	0.808		0.000	0.476		0.332	2.076	2.163	
Concave	1.000	0.855	0.146	0.343	0.476	0.854	0.379	2.369		3.143
Zero	1.000	0.808		0.000	0.476		0.332	2.076	2.163	

Table 5: Equilibria for different values of η in the Non-Linear Model. Parameters: $\beta = 1, \rho = 0.05, d = 2, \bar{h} = 0.5, b = 0.16$.

The impact of η on water quality and social utility. Reducing the environmental impact of fertilizers by reducing η , encourages fertilizer use, which in turn lowers water quality and raises the aquifer level due to increased agricultural production.

In these simulations, the Non-Linear Model consistently produces higher utility than the no-fertilizer benchmark and outperforms the cases with varying β at fixed η .

The aquifer level is generally above the socially desired threshold. Simulation results consistently show that the aquifer level exceeds the socially optimal level \bar{h} across all considered cases. This outcome highlights how even partial reductions in the pollutants generated by fertilizers—possibly achieved through technological improvements—can make fertilizer use more appealing. As a result, agricultural productivity increases, but water quality deteriorates.

Figures 7 and 8 illustrate the dynamic trajectories associated with high and low η , respectively.

Figure 7: Optimal paths in the Non-Linear Model for $\eta = 0.9$, $\beta = 0.85$

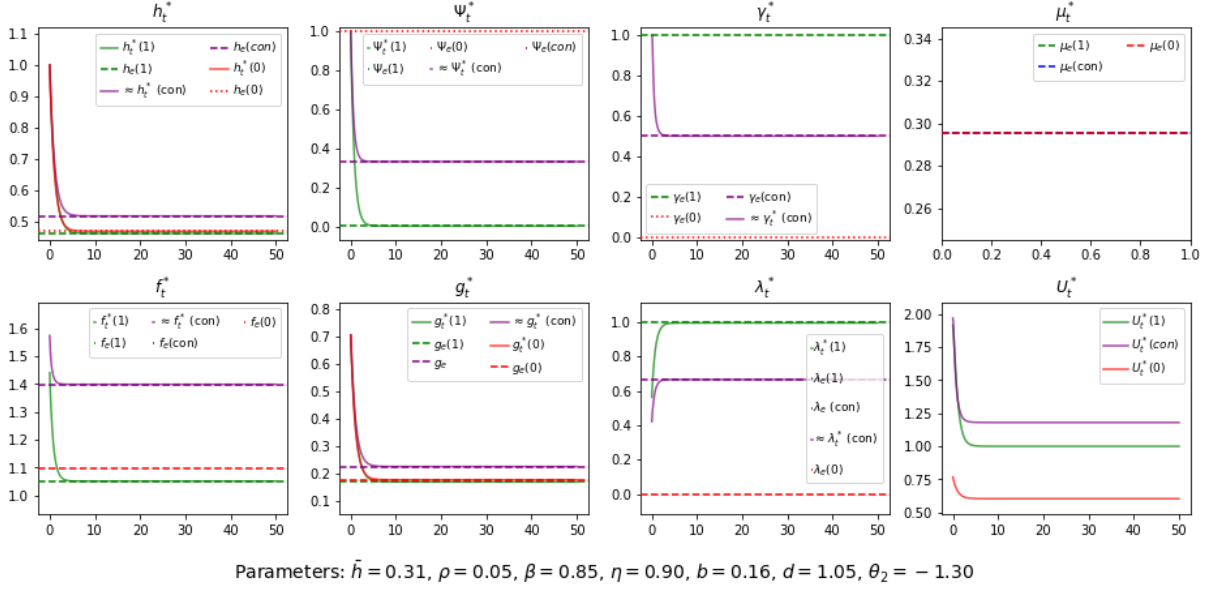
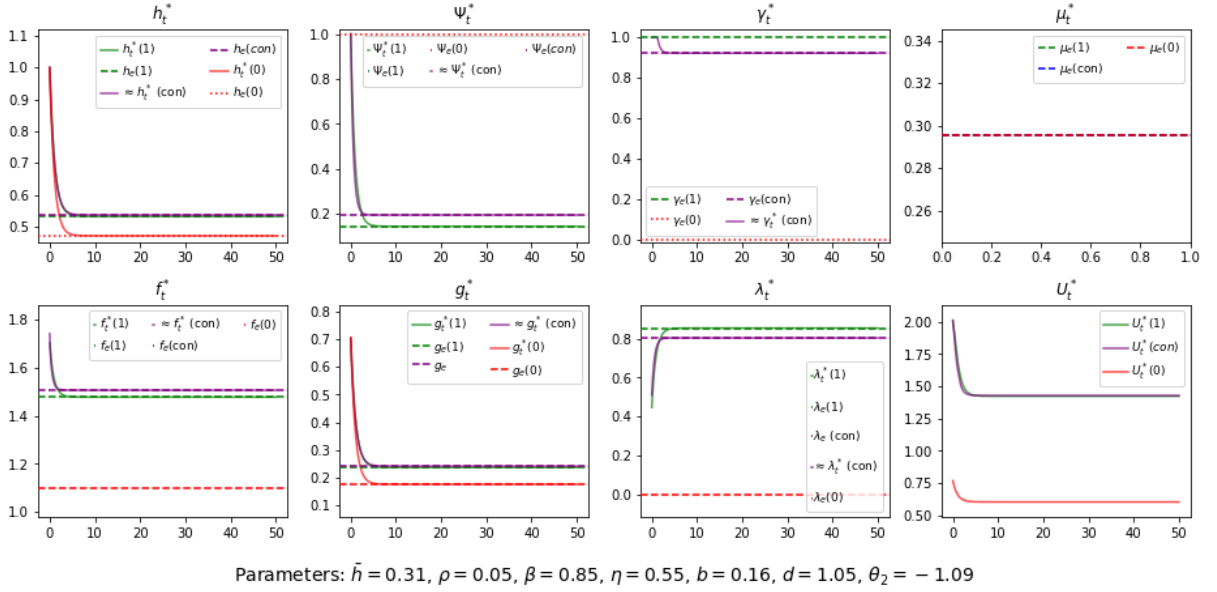
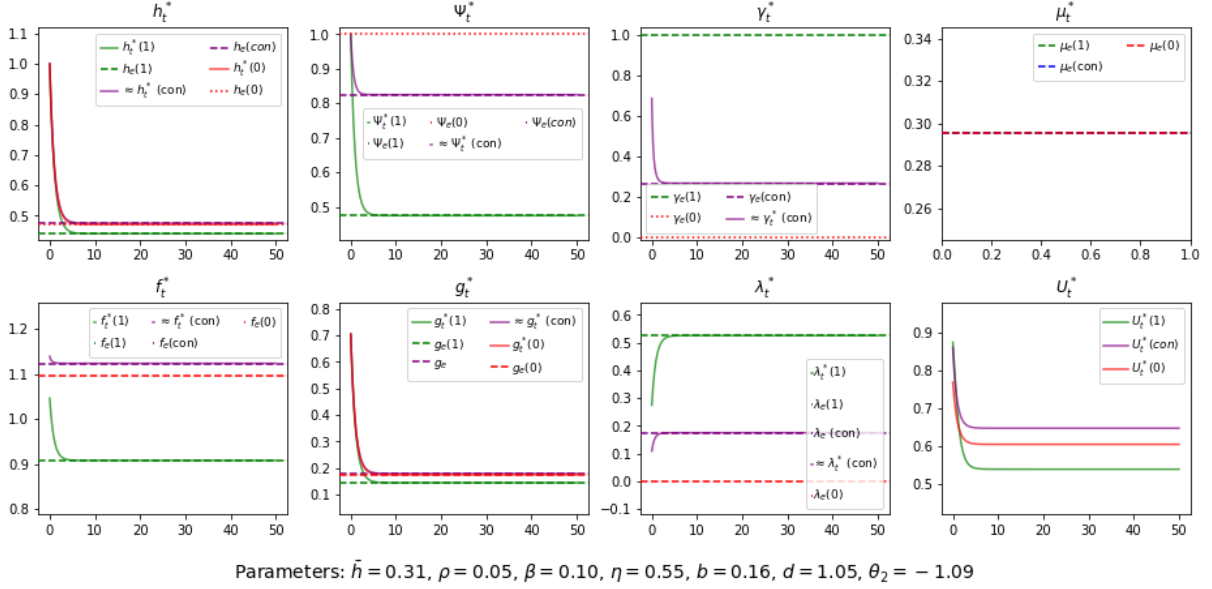


Figure 8: Optimal paths in the Non-Linear Model for $\eta = 0.55$, $\beta = 0.85$



Comparing Figures 7 and 8 shows that social utility in both fertilizer-based models increases as the pollution coefficient η decreases, reflecting the reduced environmental cost of fertilizer use. Furthermore, these figures illustrate that the gap between the utility trajectories in the Non-Linear and Full Fertilizer Models narrows as η declines and, consequently, fertilizer use in the Non-Linear Model rises—driven by the lower marginal damage associated with fertilizer application. As γ_t approaches 1, both models converge in behavior and performance. Conversely, for higher values of η , γ_e remains below this threshold (e.g., when $\eta = 0.9$, $\gamma_e \approx 0.5$), the utility in the Non-Linear Model stays lower, though the difference progressively diminishes as η decreases and fertilizer use intensifies.

Figure 9: Optimal paths in the Non-Linear Model for $\eta = 0.55$, $\beta = 0.1$



An analysis of the trajectory of λ_t reveals how fluctuations in fertilizer-generated pollutants or food rebates influence the shadow price of water quality. As discussed in Section 4.3 this shadow price reflects the marginal cost of preserving water quality in the presence of fertilizer use. When the pollution parameter η decreases—as shown in Figures 7 and 8—the environmental cost of fertilizers is reduced, resulting in lower values of λ_t .

In contrast, when β increases (see Figures 8 and 9), the marginal cost of water quality increases, as the gains from food production no longer offset the environmental degradation. Consequently, the shadow price, λ_t , mirrors the trade-off between agricultural growth and environmental sustainability, highlighting the increasing opportunity cost of further fertilizer application.

Further sensitivity Analysis of the Non-Linear Model.

We present a final set of simulations examining the impact of changes in β within the Non-Linear Model. Table 6 reports the values of β for which the parametric constraints of all three models are satisfied, enabling a direct comparison. Table 7 covers cases where the conditions of the Non-Linear Model are not fulfilled. Finally, Table 8 identifies the range of β values for which the optimal strategy involves no fertilizer use.

Scenario	β	h_e	Ψ_e	γ_e	μ_e	λ_e	g_e	f_e	$U^e(1)$	$U^e(0)$	U_e
Concave	0.2	0.803	0.689	0.646	0.467	0.311	0.336	1.121			0.642
Full	0.2	0.785	0.545	1	0.467	0.455	0.317	1.058	0.659		
No	0.2	0.779		0	0.467		0.312	1.040		0.551	
Concave	0.3	0.820	0.586	0.819	0.467	0.414	0.353	1.176			0.775
Full	0.3	0.810	0.508	1	0.467	0.492	0.343	1.143	0.768		
No	0.3	0.779		0	0.467		0.312	1.040		0.551	

Table 6: Equilibria under valid parametric conditions in all three models. Parameters: $\eta = 0.4, \rho = 0.07, d = 0.9, \bar{h} = 0.5, b = 0.3$.

Scenario	β	h_e	Ψ_e	γ_e	μ_e	λ_e	g_e	f_e	$U^e(1)$	$U^e(0)$
Full	0.5	0.862	0.435	1	0.467	0.565	0.394	1.314	1.013	
No	0.5	0.779		0	0.467		0.312	1.040		0.551
Full	0.6	0.887	0.398	1	0.467	0.602	0.420	1.399	1.148	
No	0.6	0.779		0	0.467	0.000	0.312	1.040		0.551
Full	0.7	0.913	0.361	1	0.467	0.639	0.445	1.485	1.292	
No	0.7	0.779		0	0.467	0.000	0.312	1.040		0.551
Full	0.8	0.938	0.325	1	0.467	0.675	0.471	1.570	1.444	
No	0.8	0.779		0	0.467	0.000	0.312	1.040		0.551
Full	0.9	0.964	0.288	1	0.467	0.712	0.497	1.655	1.604	
No	0.9	0.779		0	0.467	0.000	0.312	1.040		0.551
Full	1	0.990	0.251	1	0.467	0.749	0.522	1.741	1.773	
No	1	0.779		0	0.467	0.000	0.312	1.040		0.551

Table 7: Equilibria when the Non-Linear Model’s parametric restrictions are not satisfied. Parameters: $\eta = 0.4, \rho = 0.07, d = 0.9, \bar{h} = 0.5, b = 0.3$.

Scenario	β	h_e	γ_e	μ_e	g_e	f_e	$U^e(1)$	$U^e(0)$
No	0.050	0.779	0	0.467	0.312	1.040	0.510	0.551
No	0.000	0.779	0	0.467	0.312	1.040	0.465	0.551
No	0.160	0.779	0	0.467	0.312	1.040	0.617	0.551
No	0.400	0.779	0	0.467	0.312	1.040	0.887	0.551

Table 8: Equilibria where full fertilizer use is suboptimal. Parameters: $\eta = 0.4, \rho = 0.07, d = 0.9, \bar{h} = 0.5, b = 0.3$.

5.3 Results discussion

The analysis conducted in this paper demonstrates the usefulness of deterministic dynamic models for evaluating the long-term impact of fertilizer use on aquifer systems. By incorporating key environmental and economic parameters, the models enable a comprehensive assessment of optimal societal decisions concerning food production, water consumption, and fertilizer application, along with their effects on aquifer water quality and depth.

The two proposed models—linear and non-linear—enable a structured comparison between three different scenarios: (i) no fertilizer use, following the benchmark model of Martin and Stahn (2013); (ii) full fertilizer application; and (iii) intermediate fertilizer use levels resulting from concave price discounting. These models are flexible enough to identify under which combinations of parameters each scenario emerges as optimal in terms of social utility.

Moreover, the framework allows for the exploration of how parametric variations influence model outcomes, offering insights into plausible real-world dynamics in aquifers with similar characteristics. These simulations facilitate the design and evaluation of targeted environmental and agricultural policies, such as reducing price incentives for fertilizer use or mitigating the pollutants generated by agricultural practices. The outcomes shed light on how policy choices shape optimal societal behavior and, ultimately, the trade-off between environmental preservation and economic efficiency.

With respect to the conditions under which fertilizer use is not socially desirable, the Linear Model shows that negative price rebates (or even moderate positive when the environmental impact of fertilizers is high) are necessary to discourage fertilizer application. The Linear Model also underscores the role of environmental resilience in shaping long-term outcomes. As the natural absorption capacity δ decreases, the relative difference in utility between the fertilizer-based and the no-fertilizer models grows, with the latter becoming comparatively more advantageous. This highlights the importance of environmental degradation rates in evaluating policy alternatives.

In the Non-Linear Model, numerical simulations evidence that increasing price discounts and decreasing pollution per unit of fertilizer contribute to higher fertilizer use. However, even when water quality deteriorates substantially, the optimal level fertilizer remain moderate—well below the maximum threshold. This reflects a built-in precautionary behavior in the model structure, offering a more realistic depiction of decision-making under environmental constraints.

Importantly, the Non-Linear Model outperforms the Linear Model with full fertilizer use in intermediate scenarios, where neither the pollution load nor the price discount is extreme. In these contexts, moderate fertilizer use maximizes social welfare more effectively than the two polar alternatives.

If the primary goal is to preserve water quality, minimizing food price discounts associated with fertilizer use is more effective than attempting to reduce the pollutants themselves. The latter strategy tends to incentivize fertilizer use, thus increasing environmental pressure.

The models suggest that society exhibits a higher elasticity in pollutant-fertilizer consumption, meaning that increases or decreases in pollutants lead to proportional changes in fertilizer use. Conversely, the impact of food price rebates is more dependent on pollution levels, requiring larger discounts to incentivize fertilizer use when pollution is high.

Finally, from a policy standpoint, raising awareness of the environmental externalities of fertilizers, and promoting innovations that reduce their harmful effects, appears to be a more efficient strategy than providing price incentives for conventional agricultural production.

In summary, our results indicate that intermediate fertilizer use consistently leads to higher social welfare than zero or full fertilizer application. However, it is important to emphasize that these results are grounded in numerical simulation and contingent on the specific assumptions and parameter values used.

6 Limitations and Further work

This study has several limitations inherent to its theoretical and numerical nature. The models developed focus exclusively on fertilizer use in agriculture, providing a framework for analyzing the long-term impacts of such practices on aquifer systems. While the models yield valuable insights into policy evaluation and water quality dynamics, the conclusions are conditional on the model assumptions and parameter values.

For instance, the representation of social utility in the model adopts a generic formulation that does not explicitly account for stakeholder-specific preferences, such as those of farmers, whose objectives may differ from those of society as a whole (Liu et al., 2018; Pan et al., 2020).

To facilitate a direct comparison with the benchmark model by Martin and Stahn (Martin & Stahn, 2013), the parameter values used here were deliberately chosen to align with

or remain close to those in the reference framework. While this enhances comparability, future work should incorporate empirical data to validate the results and improve the model’s applicability to real-world settings.

For example, parameter calibration based on observed data from a specific geographical area could provide more realistic insights. In addition, the sensitivity of model dynamics to variations in natural degradation capacity deserves further exploration, particularly in light of the assumptions made regarding the discount rate.

Finally, it is also important to note that the current models attribute aquifer contamination exclusively to fertilizer use. In practice, groundwater pollution is shaped by a broader set of factors, including saline intrusion, wastewater discharge, and soil aridity (Gorelick & Zheng, 2015). Expanding the model to incorporate these elements, as well as Managed Aquifer Recharge (MAR) strategies, could offer a more comprehensive understanding of water quality dynamics.

7 Conclusions

This paper has addressed the management of groundwater resources in the context of fertilizer-dependent agriculture, with particular attention to its impact on aquifer water quality and depth. To this end, two dynamic models based on optimal control theory were developed, building on the benchmark framework proposed by Martin and Stahn (Martin & Stahn, 2013).

The study contributes to the literature on groundwater pollution by modeling fertilizer use as both a source of environmental degradation and a mechanism for lowering food prices through reduced production costs. While fertilizers may offer economic advantages over organic alternatives, they also entail significant environmental costs due to water contamination, which necessitates treatment and management.

The two models differ in how they represent the cost-reduction effect of fertilizers. The Linear Model assumes an all-or-nothing approach to fertilizer use, while the Non-Linear Model introduces a concave discount structure that allows for interior optima. This distinction enables a richer analysis of policy scenarios and equilibrium outcomes.

The analytical and numerical resolution of the models, based on the Maximum Principle and complemented by Hartman’s linearization, has allowed for a precise characterization of equilibrium behavior under different policy and environmental scenarios.

A series of simulations based on the parameter set from Martin and Stahn was carried out to evaluate how changes in price discounts and pollution levels affect system dynamics and social welfare. Simulation 1 explored the effects of fertilizer-induced food price reductions in the Linear Models. Simulations 2 and 3 focused on the Non-Linear Model, analyzing the optimal fertilizer levels under varying discount rates and the effects of changes in pollutant intensity per unit of fertilizer applied.

The analysis of the Linear Model revealed the conditions under which full or zero fertilizer use emerges as optimal. These outcomes depend critically on the pollution level, the natural degradation capacity, and the strength of price incentives. When natural absorption is high and pollution is low, full fertilizer use can be socially desirable. Conversely, steep price discounts may promote fertilizer use even when it is environmentally detrimental.

The results of the Non-Linear Model indicate that intermediate levels of fertilizer use can yield higher social utility than either of the two extremes. Even under substantial

deterioration of water quality, optimal fertilizer application remains below the maximum threshold, suggesting a precautionary behavior embedded in the model.

To address the challenges posed by climate change, it is advisable to implement policies aimed at reducing the price differential between organic and conventional agricultural practices. Narrowing this gap would help curb fertilizer use by making sustainable alternatives more economically viable. One promising avenue is investment in research and development to lower the production costs associated with non-polluting methods. This is particularly relevant given that organic products tend to be more expensive due to their inherently higher production costs (FAO, 2024; Redlichová et al., 2021; Wilson & Tisdell, 2001).

Alternatively, targeting the pollutant intensity of fertilizer use may prove more effective than modifying price incentives. The models suggest that fertilizer use is more responsive to changes in pollution levels than to changes in food price discounts. Thus, mitigating environmental damage at the source could yield greater improvements in welfare while exerting less pressure on water resources.

Ultimately, the proposed models generalize the benchmark case by Martin and Stahn and replicate its results when no fertilizers are applied. They offer a versatile tool for evaluating environmental and agricultural policies aimed at balancing sustainability and economic efficiency in aquifer systems.

While the models show promise for policy analysis in aquifers with similar characteristics, it is important to acknowledge their limitations. The findings are contingent on the theoretical structure and parameter assumptions, and may not generalize without empirical validation. Future research should expand the empirical basis of the models, conduct more comprehensive parametric analyses, and explore the existence of turnpike properties to strengthen the robustness of the conclusions.

Acknowledgements

Marta Llorente acknowledge financial support from UCM-Santander project PR3/23-30830.

References

- Alam, S., Borthakur, A., Ravi, S., Gebremichael, M., & Mohanty, S. K. (2021). Managed aquifer recharge implementation criteria to achieve water sustainability. *Science of The Total Environment*, 768, 144992. Retrieved from <https://www.sciencedirect.com/science/article/pii/S0048969721000589> doi: 10.1016/j.scitotenv.2021.144992
- Anderson, B. A., Romani, J. H., Phillips, H., Wentzel, M., & Tlabela, K. (2007). Exploring environmental perceptions, behaviors and awareness: water and water pollution in south africa. *Population and Environment*, 28, 133–161. Retrieved from <https://doi.org/10.1007/s11111-007-0038-5> doi: 10.1007/s11111-007-0038-5
- Bijay-Singh, & Craswell, E. (2021). Fertilizers and nitrate pollution of surface and ground water: an increasingly pervasive global problem. *SN Applied Sciences*, 3(4), 518. Retrieved from <https://doi.org/10.1007/s42452-021-04521-8> doi: 10.1007/s42452-021-04521-8
- Brock, W. A., Xepapadeas, A., & Yannacopoulos, A. N. (2014). Optimal control in space and time and the management of environmental resources. *Annual Review of Resource Economics*, 6(1), 47-49. Retrieved from <https://www.annualreviews.org/content/journals/10.1146/annurev-resource-100913-012411> doi: 10.1146/annurev-resource-100913-012411
- Carson, R., & Tran, B. (2009, 11). Discounting behavior and environmental decisions. *Journal of Neuroscience, Psychology, and Economics*, 2, 112-130. doi: 10.1037/a0017685
- Corral-Verdugo, V., Frias-Armenta, M., Pérez-Urias, F., Orduña-Cabrera, V., & Espinoza-Gallego, N. (2002). Residential water consumption, motivation for conserving water and the continuing tragedy of the commons. *Environmental management*, 30, 527–535. Retrieved from <https://doi.org/10.1007/s00267-002-2599-5> doi: 10.1007/s00267-002-2599-5
- Dillon, P., Stuyfzand, P., Grischek, T., Lluria, M., Pyne, R. D. G., Jain, R. C., ... Sapiano, M. (2019). Sixty years of global progress in managed aquifer recharge. *Hydrogeology Journal*, 27(1), 1-30. Retrieved from <https://doi.org/10.1007/s10040-018-1841-z> doi: 10.1007/s10040-018-1841-z
- FAO. (2024). *Why is organic food more expensive than conventional food?* Retrieved from <http://www.fao.org/organicag/oa-faq/oa-faq5/en/> (Retrieved on 26 May 2024)
- Gorelick, S. M., & Zheng, C. (2015). Global change and the groundwater management challenge. *Water Resources Research*, 51(5), 3031-3051. Retrieved from <https://agupubs.onlinelibrary.wiley.com/doi/abs/10.1002/2014WR016825> doi: <https://doi.org/10.1002/2014WR016825>
- Guo, L., Li, H., Cao, X., Cao, A., & Huang, M. (2021). Effect of agricultural subsidies on the use of chemical fertilizer. *Journal of Environmental Management*, 299, 113621. Retrieved from <https://www.sciencedirect.com/science/article/pii/S0301479721016832> doi: 10.1016/j.jenvman.2021.113621
- Hardin, G. (1968). The tragedy of the commons. *Science*, 162(3859), 1243-1248. Retrieved from <https://www.science.org/doi/abs/10.1126/science.162.3859.1243> doi: 10.1126/science.162.3859.1243
- Hartman, P., & Wintner, A. (1953). On the local behavior of solutions of non-parabolic partial differential equations. *American Journal of Mathematics*, 75(3), 449–476. Retrieved 2024-06-16, from <http://www.jstor.org/stable/2372496> doi: 10.2307/2372496
- Heinz, I., Salgot, M., & Dávila, J. M.-S. (2011). Evaluating the costs and benefits of water reuse and exchange projects involving cities and farmers. *Water International*, 36(4), 455-466. Retrieved from <https://doi.org/10.1080/02508060.2011.594984> doi: 10.1080/02508060.2011.594984
- Intriligator, M. D. (1975). Applications of optimal control theory in economics. *Synthese*, 31(2), 271–288. Retrieved 2024-05-29, from <https://link.springer.com/article/10.1007/>

bf00485980 doi: 10.1007/bf00485980

- Jean-Christophe, P. (2020). Conflicting objectives in groundwater management. *Water Resources and Economics*, 31, 100122. Retrieved from <https://www.sciencedirect.com/science/article/pii/S2212428417301573> doi: 10.1016/j.wre.2018.06.001
- Jodar-Abellan, A., López-Ortiz, M. I., & Melgarejo-Moreno, J. (2019). Wastewater treatment and water reuse in Spain. current situation and perspectives. *Water*, 11(8). Retrieved from <https://www.mdpi.com/2073-4441/11/8/1551> doi: 10.3390/w11081551
- Levintal, E., Kniffin, M. L., Ganot, Y., Marwaha, N., Murphy, N. P., & Dahlke, H. E. (2023). Agricultural managed aquifer recharge (ag-mar)—a method for sustainable groundwater management: a review. *Critical Reviews in Environmental Science and Technology*, 53(3), 291–314. Retrieved from <https://doi.org/10.1080/10643389.2022.2050160> doi: 10.1080/10643389.2022.2050160
- Liu, T., Bruins, R. J. F., & Heberling, M. T. (2018). Factors influencing farmers' adoption of best management practices: A review and synthesis. *Sustainability*, 10(2). Retrieved from <https://www.mdpi.com/2071-1050/10/2/432> doi: 10.3390/su10020432
- Manzoor, T., Aseev, S., Rovenskaya, E., & Muhammad, A. (2014). Optimal control for sustainable consumption of natural resources. *IFAC Proceedings Volumes*, 47(3), 10725–10730. Retrieved from <https://www.sciencedirect.com/science/article/pii/S1474667016433185> (19th IFAC World Congress) doi: 10.3182/20140824-6-ZA-1003.01474
- Marena, M., & Montrucchio, L. (1999). Neighborhood turnpike theorem for continuous-time optimization models. *Journal of optimization theory and applications*, 101, 651–676. Retrieved from <https://link.springer.com/article/10.1023/A:1021794221688> doi: 10.1023/A:1021794221688
- Martin, E., & Stahn, H. (2013). Potential conflict and inefficiencies arising in agri-environmental management. *Journal of Agricultural Economics*, 64(2), 423–445. Retrieved from <https://doi.org/10.1111/j.1477-9552.2012.00374.x> doi: 10.1111/j.1477-9552.2012.00374.x
- MITECO. (2023, September 9). *El 14,6% del territorio está en emergencia por escasez de agua y el 27,4%, en alerta.* (<https://www.miteco.gob.es/es/prensa/ultimas-noticias/2023/09>)
- MITECO. (2024, May 5). *La reserva hídrica española se encuentra al 66,3% de su capacidad.* (<https://www.miteco.gob.es/es/prensa/ultimas-noticias/2024/mayo>)
- Nahorski, Z., & Ravn, H. F. (2000). A review of mathematical models in economic environmental problems. *Annals of operations research*, 97, 165–179. Retrieved from <https://doi.org/10.1023/A:1018913316076> doi: 10.1023/A:1018913316076
- Page, D., Bekele, E., Vanderzalm, J., & Sidhu, J. (2018). Managed aquifer recharge (mar) in sustainable urban water management. *Water*, 10(3). Retrieved from <https://www.mdpi.com/2073-4441/10/3/239> doi: 10.3390/w10030239
- Pan, D., He, M., & Kong, F. (2020). Risk attitude, risk perception, and farmers' pesticide application behavior in China: A moderation and mediation model. *Journal of Cleaner Production*, 276, 124241. Retrieved from <https://www.sciencedirect.com/science/article/pii/S0959652620342864> doi: <https://doi.org/10.1016/j.jclepro.2020.124241>
- Pavelic, P., Hoanh, C. T., D'haeze, D., Vinh, B. N., Viossanges, M., Chung, D. T., ... Ross, A. (2022). Evaluation of managed aquifer recharge in the central highlands of Vietnam. *Journal of Hydrology: Regional Studies*, 44, 101257. Retrieved from <https://www.sciencedirect.com/science/article/pii/S2214581822002701> doi: 10.1016/j.ejrh.2022.101257
- Polasky, S., & Dampha, N. K. (2021). Discounting and global environmental change [Journal Article]. *Annual Review of Environment and Resources*, 46(Volume 46, 2021), 691–717. Retrieved from <https://www.annualreviews.org/content/journals/10.1146/annurev-environ-020420-042100> doi: <https://doi.org/10.1146/annurev>

- Redlichová, R., Chmelíková, G., Blažková, I., Svobodová, E., & Vanderpuje, I. N. (2021). Organic food needs more land and direct energy to be produced compared to food from conventional farming: Empirical evidence from the czech republic. *Agriculture*, 11(9). Retrieved from <https://www.mdpi.com/2077-0472/11/9/813> doi: 10.3390/agriculture11090813
- Roseta-Palma, C. (2003). Joint quantity/quality management of groundwater. *Environmental and Resource Economics*, 26(1), 89-106. Retrieved from <https://doi.org/10.1023/A:1025681520509> doi: 10.1023/A:1025681520509
- Sethi, S. P. (2019). *What is optimal control theory?* Cham: Springer International Publishing. Retrieved from https://doi.org/10.1007/978-3-319-98237-3_1 doi: 10.1007/978-3-319-98237-3_1
- Singh, S., Anil, A. G., Kumar, V., Kapoor, D., Subramanian, S., Singh, J., & Ramamurthy, P. C. (2022). Nitrates in the environment: A critical review of their distribution, sensing techniques, ecological effects and remediation. *Chemosphere*, 287, 131996. Retrieved from <https://www.sciencedirect.com/science/article/pii/S0045653521024681> doi: 10.1016/j.chemosphere.2021.131996
- Tran, K. C., Euan, J., & Isla, M. L. (2002). Public perception of development issues: impact of water pollution on a small coastal community. *Ocean & Coastal Management*, 45(6), 405-420. Retrieved from <https://www.sciencedirect.com/science/article/pii/S0964569102000777> doi: [https://doi.org/10.1016/S0964-5691\(02\)00077-7](https://doi.org/10.1016/S0964-5691(02)00077-7)
- United Nations. (2024). *Water and climate change*. Retrieved from <https://www.unwater.org/water-facts/water-and-climate-change#:~:text=Extreme%20weather%20events%20are%20making,access%20to%20water%20and%20sanitation>. (Retrieved on June 2024.)
- Uri, N. D. (1997). Incorporating the environmental consequences in the fertilizer use decision. *Science of The Total Environment*, 201(2), 99-111. Retrieved from <https://www.sciencedirect.com/science/article/pii/S0048969797000880> doi: 10.1016/S0048-9697(97)00088-0
- Weersink, A., Livernois, J., Shogren, J. F., & Shortle, J. S. (1998). Economic instruments and environmental policy in agriculture. *Canadian Public Policy / Analyse de Politiques*, 24(3), 309-327. Retrieved from <http://www.jstor.org/stable/3551971> doi: 10.2307/3551971
- Wilson, C., & Tisdell, C. (2001). Why farmers continue to use pesticides despite environmental, health and sustainability costs. *Ecological Economics*, 39(3), 449-462. Retrieved from <https://www.sciencedirect.com/science/article/pii/S0921800901002385> doi: 10.1016/S0921-8009(01)00238-5
- World Bank. (2023). *Water*. Retrieved from <https://www.worldbank.org/en/topic/water>
- Yadav, S. N. (1997). Dynamic optimization of nitrogen use when groundwater contamination is internalized at the standard in the long run. *American Journal of Agricultural Economics*, 79(3), 931-945. Retrieved from <https://doi.org/10.2307/1244433> doi: 10.2307/1244433
- Yang, X.-S. (2017). Chapter 20.3 - newton raphson method. In X.-S. Yang (Ed.), *Engineering mathematics with examples and applications* (p. 231-241). Academic Press. Retrieved from <https://www.sciencedirect.com/science/article/pii/B9780128097304000276> doi: 10.1016/B978-0-12-809730-4.00027-6

8 Appendix

A Proof of Proposition 4

Proof. To verify the first-order conditions specified by the Pontryagin's Maximum Principle (see Theorem 1), we define the current-value Hamiltonian for the linear problem (19) with $D(\gamma_t) = \beta\gamma_t$ as:

$$H_1(h_t, \Psi_t, f_t, g_t, \gamma_t, \lambda_t, \mu_t) = U_1(h_t, \Psi_t, f_t, g_t, \gamma_t) + \mu_t(bf_t - g_t) + \lambda_t[\delta(1 - \Psi_t) - \eta f_t \gamma_t].$$

Using (18), this expression can be rewritten as:

$$\begin{aligned} H_1(h_t, \Psi_t, f_t, g_t, \gamma_t, \lambda_t, \mu_t) &= U_0(h_t, f_t, g_t) + \beta\gamma_t f_t - \frac{1}{2}(1 - \Psi_t)^2 + \mu_t(bf_t - g_t) \\ &\quad + \lambda_t[\delta(1 - \Psi_t) - \eta f_t \gamma_t] = \\ &= H_0(h_t, f_t, g_t, \mu_t) + \beta\gamma_t f_t - \frac{1}{2}(1 - \Psi_t)^2 + \lambda_t[\delta(1 - \Psi_t) - \eta f_t \gamma_t], \end{aligned} \quad (\text{A.1})$$

where

$$H_0(h_t, f_t, g_t, \mu_t) = U_0(h_t, f_t, g_t) + \mu_t(bf_t - g_t)$$

is the current value Hamiltonian for the benchmark problem:

$$\begin{cases} \max_{f_t, g_t} \int_0^\infty U_0(h_t, f_t, g_t) e^{-\rho t} dt & \rho \in [0, 1] \\ \text{s.t.} & \dot{h}_t = bf_t - g_t, \quad h_0 = 1, \quad h_t \in (0, 1). \end{cases} \quad (\text{A.2})$$

The optimal intertemporal paths of problem (A.2), as derived in Martin and Stahn (2013), are given by:

$$\begin{aligned} f_t^* &= d + \frac{b\bar{h}}{1 + \rho}, \quad g_t^* = g^e(0) + (1 - h^e(0))e^{-t}, \\ h_t^* &= h^e(0) + (1 - h^e(0))e^{-t}, \quad \mu_t^* = \frac{\bar{h}}{\rho + 1}, \end{aligned} \quad (\text{A.3})$$

where:

$$g^e(0) = bd + \frac{\bar{h}b^2}{\rho + 1} \quad \text{and} \quad h^e(0) = bd + \frac{\bar{h}(b^2 + 1)}{\rho + 1},$$

From Theorem 1-(iii), it follows that:

$$H_0(h_t^*, f_t^*, g_t^*, \mu_t^*) \geq H_0(h_t^*, f_t, g_t, \mu_t^*) \quad (\text{A.4})$$

for any admissible control pair (f_t, g_t) . Now, by setting $\gamma_t^* = 0$, $\Psi_t^* = 1$, $\lambda_t^* = 0$, we obtain

$$H_1(h_t^*, \Psi_t^*, f_t^*, g_t^*, \gamma_t^*, \lambda_t^*, \mu_t^*) = H_0(h_t^*, f_t^*, g_t^*, \mu_t^*). \quad (\text{A.5})$$

Suppose that $\beta < 0$, combining (A.5), (A.4) and (A.1) yields:

$$\begin{aligned} H_1(h_t^*, \Psi_t^*, f_t^*, g_t^*, \gamma_t^*, \lambda_t^*, \mu_t^*) &= H_0(h_t^*, f_t^*, g_t^*, \mu_t^*) \geq H_0(h_t^*, f_t, g_t, \mu_t^*) = \\ &= H_1(h_t^*, \Psi_t^*, f_t, g_t, \gamma_t, \lambda_t^*, \mu_t^*) - \beta\gamma_t f_t \geq H_1(h_t^*, \Psi_t^*, f_t, g_t, \gamma_t, \lambda_t^*, \mu_t^*), \end{aligned}$$

which proves that the controls (h_t^*, Ψ_t^*) satisfy condition (iii) of Theorem 1 for the adjoint variables λ_t^* and μ_t^* .

Condition (i) holds trivially. To verify condition (ii), we use the optimality of the paths $(h_t^*, f_t^*, g_t^*, \mu_t^*)$ and the relation in (A.1), to obtain

$$\dot{\mu}_t^* = \rho\mu_t^* - \frac{\partial H_0(h_t^*, f_t^*, g_t^*, \mu_t^*)}{\partial h_t} = \rho\mu_t^* - \frac{\partial H_1(h_t^*, \Psi_t^*, f_t^*, g_t^*, \gamma_t^*, \lambda_t^*, \mu_t^*)}{\partial h_t}.$$

The equation for λ_t^* holds naturally as:

$$\dot{\lambda}_t^* = \rho\lambda_t^* - \frac{\partial H_1(h_t^*, \Psi_t^*, f_t^*, g_t^*, \gamma_t^*, \lambda_t^*, \mu_t^*)}{\partial \Psi_t} = 0,$$

given that $\lambda_t^* = 0$ and $\Psi_t^* = 1$.

The transversality conditions hold trivially since μ_t is constant, $\rho < 1$ and $\lambda_t = 0$.

Finally, the second-order conditions are fulfilled because the Standart Hamiltonian

$$\begin{aligned} \hat{H}(h_t, \Psi_t, \lambda_t, \mu_t) = & e^{-t\rho} \left(-\frac{1}{2}g_t^{*2} + g_t^*h_t + df_t^* - \frac{1}{2}f_t^{*2} - \frac{1}{2}(h_t - \bar{h})^2 - \frac{1}{2}(1 - \Psi_t)^2 \right) \\ & + \lambda_t\delta(1 - \Psi_t) + \mu_t[bf_t^* - g_t^*] \end{aligned} \quad (\text{A.6})$$

is concave in (h_t, Ψ_t) . □

B Proof of Proposition 5

Proof. Let $\beta > 0$ and suppose that

$$\mu^e = \frac{\bar{h}}{2 - \delta} < \min\{m_1 =: \frac{\eta^2 + \delta - \delta b(\beta + d)}{\eta^2 + \delta(1 + b^2)}, m_2 =: \frac{\eta^2 + \delta - \eta(\beta + d)}{\eta b}\}. \quad (\text{B.1})$$

Define the current-value Hamiltonian of problem (19) with $D(\gamma_t) = \beta\gamma_t$ as:

$$\begin{aligned} H_1(h_t, \Psi_t, f_t, g_t, \gamma_t, \lambda_t, \mu_t) = & -\frac{1}{2}g_t^2 + g_th_t + (d + \beta\gamma_t)f_t - \frac{1}{2}f_t^2 - \frac{1}{2}(h_t - \bar{h})^2 \\ & + -\frac{1}{2}(1 - \Psi_t)^2 + \lambda_t[\delta(1 - \Psi_t) - \eta f_t\gamma_t] + \mu_t(bf_t - g_t). \end{aligned}$$

Let $\gamma_t^* = \text{bang}[1, 0; \lambda_t - \frac{\beta}{\eta}]$ (see (21)). According to the first-order conditions from the Maximum Principle (Theorem 1), the optimal solution $\vec{e}^*(\gamma_t^*) = \vec{e}^* := (h_t^*, \Psi_t^*, f_t^*, g_t^*, \gamma_t^*, \lambda_t, \mu_t)^5$ satisfies:

$$\begin{aligned} \frac{\partial H_1}{\partial f_t}(\vec{e}^*) = 0 & \iff d + \beta\gamma_t^* - f_t^* - \lambda_t\eta\gamma_t^* + \mu_t b = 0 \\ \frac{\partial H_1}{\partial g_t}(\vec{e}^*) = 0 & \iff h_t^* - g_t^* - \mu_t = 0 \\ \dot{\mu}_t = \rho\mu_t - \frac{\partial H_1}{\partial h_t}(\vec{e}^*) & \iff \rho\mu_t - \dot{\mu}_t = g_t^* - h_t^* + \bar{h} \\ \dot{\lambda}_t = \rho\lambda_t - \frac{\partial H_1}{\partial \Psi_t}(\vec{e}^*) & \iff \rho\lambda_t - \dot{\lambda}_t = 1 - \Psi_t^* - \lambda_t\delta \\ & \dot{h}_t^* = bf_t^* - g_t^* \\ & \dot{\Psi}_t^* = \delta(1 - \Psi_t^*) - \eta\gamma_t^*f_t^* \end{aligned} \quad (\text{B.2})$$

⁵For simplicity, we omit the explicit dependence of the steady state and optimal paths on γ_t^* in the notation, except when it is necessary for the calculations.

Substituting $\delta = 1 - \rho$, this leads to the following dynamical system

$$\begin{pmatrix} \dot{h}_t \\ \dot{\Psi}_t \\ \dot{\mu}_t \\ \dot{\lambda}_t \end{pmatrix} = \begin{pmatrix} b(d + \beta\gamma_t^*) \\ 1 - \rho - \eta\gamma_t^*(d + \beta\gamma_t^*) \\ -\bar{h} \\ -1 \end{pmatrix} + \begin{pmatrix} -1 & 0 & b^2 + 1 & -\gamma_t^*b\eta \\ 0 & \rho - 1 & -\eta\gamma_t^*b & (\gamma_t^*\eta)^2 \\ 0 & 0 & \rho + 1 & 0 \\ 0 & 1 & 0 & 1 \end{pmatrix} \begin{pmatrix} h_t^* \\ \Psi_t^* \\ \mu_t^* \\ \lambda_t^* \end{pmatrix}. \quad (\text{B.3})$$

The steady state $(h^e(\gamma_t^*), \Psi^e(\gamma_t^*), \mu^e(\gamma_t^*), \lambda^e(\gamma_t^*)) = (h^e, \Psi^e, \mu^e, \lambda^e)$ of (B.3), given by

$$\begin{aligned} h^e(\gamma_t^*) = h^e = g^e + \mu^e &= \frac{\frac{\bar{h}}{\rho+1}(1 + b^2 + \frac{(\eta\gamma_t^*)^2}{1-\rho}) + b(\beta\gamma_t^* + d)}{\frac{(\eta\gamma_t^*)^2}{1-\rho} + 1} > 0 \\ \Psi^e(\gamma_t^*) = \Psi^e &= 1 - \frac{\eta\gamma_t^*(\frac{\bar{h}}{\rho+1} + \beta\gamma_t^* + d)}{(\eta\gamma_t^*)^2 + 1 - \rho} \leq 1 \\ \mu^e(\gamma_t^*) = \mu^e &= \frac{\bar{h}}{\rho + 1} \in (0, 1) \\ \lambda^e(\gamma_t^*) = \lambda^e &= 1 - \Psi^e = \frac{\eta\gamma_t^*(\frac{\bar{h}}{\rho+1} + \beta\gamma_t^* + d)}{(\eta\gamma_t^*)^2 + 1 - \rho} \geq 0, \end{aligned} \quad (\text{B.4})$$

$$\text{where } g^e(\gamma_t^*) = g^e = bf^e = b \frac{\frac{b\bar{h}}{\rho+1} + \beta\gamma_t^* + d}{\frac{\eta^2\gamma_t^*}{1-\rho} + 1}$$

$$\text{and } f^e(\gamma_t^*) = f^e = \frac{1 - \rho}{\eta} \lambda^e = \frac{\frac{b\bar{h}}{\rho+1} + \beta\gamma_t^* + d}{\frac{\eta^2\gamma_t^*}{1-\rho} + 1},$$

is a saddle point, as the associated matrix has two positive and two negative eigenvalues. Thus, the path leading to the efficient steady state is unstable, except along the stable trajectories whose directions are given by the eigenvectors:

$$\vec{v}_1 = \begin{pmatrix} 1 \\ 0 \\ 0 \\ 0 \end{pmatrix}, \quad \vec{v}_2 = \begin{pmatrix} \frac{2b\eta\gamma_t^*}{1+\theta_2} \\ 2(1 - \theta_2) \\ 0 \\ -2 \end{pmatrix}$$

associated to the negative eigenvalues, $\theta_1 = -1$ and

$$\theta_2 = \theta_2(\gamma_t^*) = \frac{\rho - \sqrt{(2 - \rho)^2 + 4(\gamma_t^*\eta)^2}}{2} = \begin{cases} \frac{\rho - \sqrt{(2 - \rho)^2 + 4\eta^2}}{2} & \text{if } \gamma_t^* = 1 \\ \rho - 1 & \text{if } \gamma_t^* = 0. \end{cases} \quad (\text{B.5})$$

Only these stable intertemporal trajectories are admissible from an economic point of view, since they ensure that small deviations from initial conditions do not lead the system away from optimal behavior.

The stable intertemporal efficient paths satisfying the initial conditions $h_0 = 1$ and $\Psi_0 = 1$ are:

$$\begin{aligned} h_t^* &= h^e + c_1 e^{-t} + c_2 \frac{2b\eta\gamma_t^*}{1 + \theta_2} e^{\theta_2 t}, & \lambda_t^* &= \lambda^e - 2c_2 e^{\theta_2 t}, \\ \Psi_t^* &= \Psi^e + 2c_2(1 - \theta_2) e^{t\theta_2}, & f_t^* &= d + \beta\gamma_t^* - \lambda_t^*\gamma_t^*\eta + \mu^e b, \\ \mu_t &= \mu^e, & g_t^* &= h_t - \mu^e, \end{aligned} \quad (\text{B.6})$$

where the constants $c_1 = 1 - h^e - \frac{b\eta\gamma_t^*\lambda^e}{1-\theta_2^2}$ and $c_2 = \frac{1-\Psi^e}{2(1-\theta_2)} = \frac{\lambda^e}{2(1-\theta_2)}$ are derived from the initial conditions. These trajectories satisfy the transversality conditions.

To determine the optimal control γ_t^* in accordance with the bang-bang solution framework, we analyze the conditions under which $\gamma_t^* = 0$ or $\gamma_t^* = 1$ satisfies the necessary optimality criteria.

First, consider the case where $\gamma_t^* = 1$. Using the relations $h^e(1) = \mu^e(1) + \frac{b\delta}{\eta}\lambda^e(1)$ and $\lambda^e(1) = \frac{\eta(b\mu^e + \beta + d)}{\eta^2 + \delta}$, it can be shown that the condition (B.1) ensures both $h^e(1)$ and $\lambda^e(1)$ are less than one. Consequently, $h^e(1), \Psi^e(1) \in [0, 1]$. Notice that, in the specific case where $\delta b > \eta$, the minimum in (B.1) is given by m_1 .

If $\gamma_t^* = 0$, the steady states $(h^e(0), f^e(0), g^e(0), \mu^e(0))$ coincide with those presented in Martin and Stahn (2013).

Now, observe that when $\gamma_t^* = 1$, the adjoint operator $\lambda_t(1)$ as defined by (B.6) is an increasing function of $t \in (0, \infty)$ with

$$\lambda_0(1) = \frac{\theta_2(1)}{\theta_2(1) - 1} \lambda^e(1) < \lambda^e(1) \quad \text{and} \quad \lim_{t \rightarrow \infty} \lambda_t(1) = \lambda^e(1).$$

If $\beta > \eta$, then $\lambda_t(1) \leq \lambda^e(1) \leq \frac{\beta}{\eta}$ for all $t \in (0, \infty)$, because (B.1) guarantees that $\lambda_e(1) \leq 1$. In this case, the stable intertemporal efficient paths are given by (B.6) with $\gamma_t^* = 1$.

Finally, if $\beta < \eta$, it can be verified that

$$\lambda^e(1) \leq \frac{\beta}{\eta} \iff f^e(0) = \frac{b\bar{h}}{2 - \delta} + d \leq \frac{\beta\delta}{\eta^2} \quad (\text{B.7})$$

This concludes the proof of Proposition 5.

Second-order conditions are also satisfied because the standard Hamiltonian

$$\begin{aligned} \hat{H}_1(h_t, \Psi_t, \lambda_t, \mu_t) = & e^{-t\rho} \left(-\frac{1}{2}g_t^{*2} + g_t^*h_t + (d + \beta\gamma_t^*)f_t^* - \frac{1}{2}f_t^{*2} - \frac{1}{2}(h_t - \bar{h})^2 - \frac{1}{2}(1 - \Psi_t)^2 \right) \\ & + \lambda_t[\delta(1 - \Psi_t) - \eta f_t^* \gamma_t^*] + \mu_t[b f_t^* - g_t^*] \end{aligned} \quad (\text{B.8})$$

is concave in (h_t, Ψ_t) . \square

C Proof of Proposition 7

Proof. Suppose that $0 < \beta \leq 2\eta$ and that the following parametric restriction holds:

$$\frac{\beta(1 - \rho)}{2\eta^2} - \frac{\beta}{2} \leq b \frac{\bar{h}}{\rho + 1} + d \leq \min \left\{ \frac{4\eta(1 - \rho)}{\beta^2} - \frac{\beta^2}{4\eta}, \frac{1}{b} \left(1 - \frac{\bar{h}}{\rho + 1} \right) - \frac{\beta}{2} \right\} \quad (\text{C.1})$$

with $1 - \rho > \frac{\beta^4}{16\eta^2}$ and $\frac{\bar{h}}{\rho + 1} \leq 1 - \frac{b\beta}{2}$. We define the current-value Hamiltonian associated with the optimal control problem (19) with $D(\gamma_t) = \beta\gamma_t^{\frac{1}{2}}$ as:

$$\begin{aligned} H(h_t, \Psi_t, f_t, g_t, \gamma_t, \lambda_t, \mu_t) = & -\frac{1}{2}g_t^2 + g_t h_t + (d + \beta\gamma_t^{\frac{1}{2}})f_t - \frac{1}{2}f_t^2 - \frac{1}{2}(h_t - \bar{h})^2 - \frac{1}{2}(1 - \Psi_t)^2 + \\ & \lambda_t[\delta(1 - \Psi_t) - \eta f_t \gamma_t] + \mu_t[b f_t - g_t]. \end{aligned}$$

The efficient solution $\vec{e}^* := (h_t^*, \Psi_t^*, f_t^*, g_t^*, \gamma_t^*, \lambda_t, \mu_t)$ satisfies the following first-order conditions of the Maximum Principle (Theorem 1):

$$\begin{aligned}
H_{f_t}(\vec{e}^*) = 0 &\iff d + \beta\gamma_t^{*\frac{1}{2}} - f_t^* - \lambda_t\eta\gamma_t^* + \mu_t b = 0 \\
H_{g_t}(\vec{e}^*) = 0 &\iff h_t^* - g_t^* - \mu_t = 0 \\
H_{\gamma_t}(\vec{e}^*) = 0 &\iff \frac{1}{2}\beta f_t^* \gamma_t^{*-\frac{1}{2}} - \lambda_t\eta f_t^* = 0 \\
\dot{\mu}_t = \rho\mu_t - H_{h_t}(\vec{e}^*) &\iff \rho\mu_t - \dot{\mu}_t = g_t^* - h_t^* + \bar{h} \\
\dot{\lambda}_t = \rho\lambda_t - H_{\Psi_t}(\vec{e}^*) &\iff \rho\lambda_t - \dot{\lambda}_t = 1 - \Psi_t^* - \lambda_t\delta \\
&\dot{h}_t^* = b f_t^* - g_t^* \\
&\dot{\Psi}_t^* = \delta(1 - \Psi_t^*) - \eta\gamma_t^* f_t^* -
\end{aligned} \tag{C.2}$$

By setting $\delta = 1 - \rho$, we obtain the following system of equations:

$$\begin{aligned}
g_t^* &= h_t^* - \mu_t & \dot{h}_t &= b \left(d + \frac{\beta^2}{4\eta\lambda_t^*} + b\mu_t \right) - h_t^* + \mu_t \\
\gamma_t^* &= \frac{\beta^2}{4\eta^2\lambda_t^2} & \dot{\Psi}_t^* &= (1 - \rho)(1 - \Psi_t^*) - \eta \left(d + \frac{\beta^2}{4\eta\lambda_t} + b\mu_t \right) \left(\frac{\beta^2}{4\eta^2\lambda_t^2} \right) \\
f_t^* &= d + \frac{\beta^2}{4\lambda_t\eta} + b\mu_t & \dot{\mu}_t &= (1 + \rho)\mu_t - \bar{h} \\
&& \dot{\lambda}_t &= \lambda_t + \Psi_t^* - 1
\end{aligned} \tag{C.3}$$

The steady state solution $(h_e, \Psi_e, \mu_e, \lambda_e)$ of (C.3) is given by:

$$\begin{aligned}
\mu_e &= \frac{\bar{h}}{\rho+1} & h_e &= bd + \frac{b\beta}{2}\gamma_e^{1/2} + (1 + b^2)\mu_e \\
\gamma_e &= \frac{\beta^2}{4\eta^2\lambda_e^2} \iff \lambda_e = \frac{\beta}{2\eta}\gamma_e^{-1/2} & g_e &= h_e - \mu_e \\
\psi_e &= 1 - \lambda_e & f_e &= d + \frac{\beta^2}{4\lambda_e\eta} + b\mu_e \\
(d + \frac{\beta}{2}\gamma_e^{1/2} + \mu_e b) \frac{2\eta^2}{\beta(1-\rho)} \gamma_e^{3/2} - 1 &= 0.
\end{aligned} \tag{C.4}$$

Given that $\Psi_e = 1 - \lambda_e$ and $\lambda_e = \frac{\beta}{2\eta}\gamma_e^{-1/2}$, the conditions $\Psi_e, \lambda_e \in [0, 1]$ hold if $\frac{\beta^2}{4\eta^2} \leq \gamma_e \leq 1$ with $\beta > 0$.

Now, define the function

$$P(\gamma_e) := (d + \frac{\beta}{2}\gamma_e^{1/2} + \mu_e b) \frac{2\eta^2}{\beta(1-\rho)} \gamma_e^{3/2} - 1. \tag{C.5}$$

On the one hand, the parametric restrictions (C.1) ensure that $P\left(\frac{\beta^2}{4\eta^2}\right) \leq 0 \leq P(1)$. On the other hand, $P(\gamma_e)$ is continuous and increasing on $[0, 1]$, hence the Intermediate Value Theorem implies that $\gamma_e \in \left[\frac{\beta^2}{4\eta^2}, 1\right]$. Finally, it can be checked that under parametric restrictions given by (C.1) the restriction $h_e \leq 1$ holds true.

Stability around the steady state is analyzed by linearizing the system and computing the Jacobian matrix:

$$J(h_e, \Psi_e, \mu_e, \lambda_e) = \begin{pmatrix} -1 & 0 & 1 + b^2 & -b\eta\gamma_e \\ 0 & -(1 - \rho) & -b\eta\gamma_e & (\eta\gamma_e)^2 + 2(1 - \rho) \\ 0 & 0 & 1 + \rho & 0 \\ 0 & 1 & 0 & 1 \end{pmatrix}.$$

The eigenvalue structure (two positive and two negative roots) confirms that the steady state is a saddle point. This permits the construction of a two-dimensional stable manifold, along which the system converges to equilibrium from given initial conditions.

The Jacobian matrix provides crucial information about the local stability of an equilibrium point. By computing its eigenvalues, one can classify the nature of the steady state. In this case, the matrix has two positive and two negative eigenvalues, indicating that the equilibrium is a saddle point. According to Hartman's linearization theorem (Hartman & Wintner, 1953), if all eigenvalues of the Jacobian matrix have non-zero real parts—i.e., the equilibrium is hyperbolic—then the qualitative behavior of the nonlinear system in a neighborhood of that point is locally equivalent to that of the linearized system. Therefore, the system inherits the saddle structure of the linearized dynamics, and a two-dimensional stable manifold exists. This manifold corresponds to the span of the eigenvectors associated with the negative eigenvalues, and any initial condition lying within it leads the system to converge to the equilibrium. Outside this manifold, trajectories diverge.

The eigenvectors corresponding to the negative eigenvalues, $\theta_1 = -1$ and $\theta_2 = \frac{\rho - \sqrt{(\rho-2)^2 + 4W}}{2}$, are given by:

$$\vec{v}_1 = \begin{pmatrix} 1 \\ 0 \\ 0 \\ 0 \end{pmatrix}, \quad \vec{v}_2 = \begin{pmatrix} \frac{-b\eta\gamma_e}{1+\theta_2} \\ \frac{W}{1-\rho+\theta_2} \\ 0 \\ 1 \end{pmatrix},$$

where $W = (\eta\gamma_e)^2 + 2(1 - \rho)$.

Therefore, the efficient intertemporal paths satisfying the initial conditions $h_0 = 1$ and $\Psi_0 = 1$ are given by:

$$\left\{ \begin{array}{l} h_t^* = h_e + c_1 e^{-t} - \frac{b\eta\gamma_e}{1+\theta_2} c_2 e^{t\theta_2} \\ \Psi_t^* = \Psi_e + \frac{W}{1-\rho+\theta_2} c_2 e^{t\theta_2} \\ \mu_t = \mu_e \\ \lambda_t = \lambda^e(1) + c_2 e^{t\theta_2} \\ f_t^* = d + \frac{\beta^2}{4\lambda_t\eta} + b\mu_e \\ g_t^* = h_t - \mu_e \\ \gamma_t^* = \frac{\beta^2}{4\eta^2\lambda_t^2} \end{array} \right. \implies \left\{ \begin{array}{l} h_t^* = h_e + (1 - h_e)e^{-t} - \frac{b\eta\gamma_e}{1+\theta_2} c_2 (e^{\theta_2 t} - e^{-t}) \\ \Psi_t^* = \Psi_e + (1 - \Psi_e)e^{t\theta_2} \\ \mu_t = \mu_e \\ \lambda_t = \lambda_e \left(1 + \frac{1 - \rho + \theta_2}{W} e^{\theta_2 t}\right) \\ f_t^* = d + \frac{\beta^2}{4\lambda_t\eta} + b\mu_e \\ g_t^* = h_t - \mu_e \\ \gamma_t^* = \frac{\beta^2}{4\eta^2\lambda_t^2} \end{array} \right. \quad (\text{C.6})$$

where $c_1 = 1 - h_e + c_2 \frac{b\eta\gamma_e}{1+\theta_2}$ and $c_2 = \frac{(1-\rho+\theta_2)(1-\Psi_e)}{W}$ are obtained from the initial conditions $h_0 = 1$ and $\Psi_0 = 1$.

Regarding the control variable $\gamma_t^* = \frac{\beta^2}{4\eta^2\lambda_t^2}$, which must lie within $[0, 1]$, we enforce this constraint explicitly using a Karush-Kuhn-Tucker (KKT) formulation:

$$\gamma_t^* = \min \left\{ 1, \max \left\{ 0, \frac{\beta^2}{4\eta^2\lambda_t^2} \right\} \right\}.$$

The transversality conditions $\lim_{t \rightarrow \infty} e^{-\rho t} \mu_t = 0$ and $\lim_{t \rightarrow \infty} e^{-\rho t} \lambda_t = 0$ are satisfied, and the second-order conditions hold as the Standart Hamiltonian:

$$\begin{aligned}\hat{H}(h_t, \Psi_t, \lambda_t, \mu_t) = & e^{-t\rho} \left(-\frac{1}{2}g_t^{*2} + g_t^*h_t + (d + \beta\gamma_t^{*1/2})f_t^* - \frac{1}{2}f_t^{*2} - \frac{1}{2}(h_t - \bar{h})^2 - \frac{1}{2}(1 - \Psi_t)^2 \right) \\ & + \lambda_t[\delta(1 - \Psi_t) - \eta f_t^* \gamma_t^{**}] + \mu_t[b f_t^* - g_t^*]\end{aligned}\tag{C.7}$$

is concave in (h_t, Ψ_t) .

Finally, as $\beta \rightarrow 0$, the optimal fertilizer use converges to zero:

$$\lim_{\beta \rightarrow 0} \frac{\beta^2}{4\eta^2\lambda^2} = 0.\tag{C.8}$$

Accordingly, the optimal solution coincides with the benchmark model without fertilizers proposed by Martin and Stahn (2013). \square